Submitted 13.9.99

In: **Image Analysis in Biology: Methods and Applications**, 2nd. ed.
D.-P. Häder Ed., CRC Press, Boca Raton, 1999

DIGITAL LIGHT MICROSCOPY TECHNIQUES FOR THE STUDY OF LIVING CYTOPLASM

Dieter G. Weiss[1], Vladimir P. Tychinsky[2], Walter Steffen[3], and Axel Budde[3]

TABLE OF CONTENTS

---

[1]Institute for Cell Biology and Biosystems Technology, Department of Biological Sciences, University of Rostock, 18051 Rostock, Germany

[2]Moscow State Institute for Radioengineering, Electronics and Automation, MIREA, Vernadskii Prospect 78, Moscow 117454, Russia

[3]Center for Biological Visualization Techniques, Institute for Cell Biology and Biosystems Technology, Department of Biological Sciences, University of Rostock, 18051 Rostock, Germany. Present address: HaSoTec GmbH, Hardware & Software Technology, Burgwall 20, 18055 Rostock, Germany

---

I. INTRODUCTION

The cytoplasm of eukaryotic cells is highly structured. It consists of the fluid phase (cytosol) and the cytoskeleton made up from several types of proteinaceous filaments. Embedded in this so called cytomatrix, which is highly viscous in animal cells, are various kinds of membrane-bounded organelles ranging from 50 nm vesicles to the mitochondria which are up to several micrometers long. Eukaryotic cells require ATP to move actively and redistribute the organelles. The cytoskeletal filaments serve as tracks, as part of the force generating mechanism, and they organize the distribution of organelles to their places of destination.

All organelles are structurally well characterized in the fixed and dehydrated state by electron microscopy. The study of most of their details in the living cell was, however, impossible for almost all but the largest organelles due to the limited resolution of light microscopy. When using visible light, this limit is around 200 nm thus making the observation of most organelles such as secretory vesicles, synaptic vesicles, peroxisomes, small lysosomes and of essentially all cytoskeletal filaments such as actin filaments (6 nm diameter), intermediate filaments (10 nm), and microtubules (25 nm) impossible. Considerable progress in the study of cytoplasmic structures and their dynamics had, therefore, to await new techniques capable to visualize these structures, identify their chemical nature, and quantitatively analyze their dynamic behavior.

Until the beginning of the ‘80s the power of light microscopy was limited by the properties of the human eye. In the meantime, the application of suitable electronic devices in light microscopy made it not only possible to obtain images at much lower light levels as required for human vision, but also to digitize and process such microscope images in "real time", i.e. at video rates, and at high spatial resolution. This led to dramatic improvements in resolution, brightness and contrast of microscopic images. This "electronic revolution in light microscopy"[1-3] provided us with new digital techniques suitable to study living cells in many instances where previously only dehydrated material could be studied electron-microscopically.

The new quality of light microscopy emerges, if one observes the specimen instead with the human eye with a video camera connected to state-of-the-art analog and digital video processing equipment, usually working at real time. Video microscopy is, thereby, much more then just adding a camera and monitor to the microscope to share the images with a larger audience. New electronic devices other than video cameras, such as high sensitivity charge-coupled device (CCD) cameras and scanning light detector systems have been added to microscopes. The three fields

- **video-enhanced contrast microscopy** for highest resolution work,
- **video-intensified microscopy** for low light applications, and
- **electronic scanning microscopy** for confocal microscopy and 3-D imaging

differ in the type of device generating the electronic image, but all three use basically the same types of analog and digital image processing routines. While all these techniques are generally defined as **electronic light microscopy**, the first two techniques are called **video microscopy**.

Four digital light microscopy techniques, that are especially well-suited for the study of living cytoplasm are discussed in this chapter. Most of these techniques are based on video microscopy, which depends on analog and digital image processing, but they all require in addition extensive digital image processing. The term **digital light microscopy** is used here to emphasize the power of digital procedures to visualize specific parameters of the intracellular dynamics, especially movements and dynamic changes of molecules.

Quantitative data for different morphological and biochemical parameters can be recorded and calculated from digitized images in real time, i.e. at video rate, and encoded in the form of gray-shaded or pseudo-color images. These can be recorded continuously yielding video films of the intracellular events. Digital microscopy also allows multiparametric studies that yield a wealth of information that was inaccessible in the past. A synopsis of some of the present video-microscopic techniques is given in Table I.

TABLE I. PARAMETERS WHICH CAN BE MEASURED BY DIGITAL LIGHT MICROSCOPY IN LIVING CELLS OR TISSUE SLICES

I. Morphology-Based Parameters

1. Visualization of cells and cellular processes in thick tissue slices (IR VEC-DIC, anaxial illumination)[10,37,38]
2. Number, position, size, and shape parameters of free cells (e.g. video microinterferometry)[151]
3. Number, position, total area, size, and shape of organelles (organelle-specific vital dyes):[10,44] nucleus,[44,152] mitochondria,[83] endoplasmic reticulum,[16,19,81] Golgi apparatus,[82] secretory vesicles,[88,92] lysosomes,[126] endosomes[44]
4. Motion analysis of organelles and microtubules:[49,50,52] velocity, fluctuation of velocity, straightness of path, rhythmicity, directionality, pauses, contribution of Brownian motion
5. Cytoplasmic viscosity (Brownian motion) (requires microinjection)[84,126]
6. Elastic properties of organelles, microtubules, membranes, and cells[129-131]
7. Local motile activity in cells (root-mean-square average of changes of pixel brightness values)[153]
8. Determination of dry matter in free cells (video microinterferometry):[151] total dry matter, dry matter distribution, pattern of flow of dry matter
9. Measurement of forces in the microscopic and molecular domain ("magnetodrome", microscopy in controlled magnetic fields[154]), laser tweezers[29,131]

II. Biochemical Parameters

1. Thickness profile of cells (optical pathlength)[31,138,139]
2. Distribution and amount of antigens (requires microinjection or fixation): fluorescence-labeled antibodies,[43] gold-labeled antibodies (also for receptor labeling and receptor or antigen transport studies)[26,89,90]
3. Concentration of substances (monochromatic illumination):[77] concentration of free intracellular Ca^{2+}, Mg^{2+}, Zn^{2+}, K^{+}, Na^{+}, Cl^{-};[31-33,142] intracellular H^{+}-concentration (pH-value);[31,33] enzyme reactions[146] endogenous fluorescent or absorbing compounds[75]
4. Membrane potential (plasma membrane and endomembranes)[155,156]
5. Metabolites can be measured by coupled bioluminescence assays; "metabolic imaging" (requires frozen sections or microinjection):[93,94] lactate, glucose, ATP
6. Intracellular metabolites and messengers can be photoactivated[157]
7. Intracellular diffusion[144]
8. Transfer of fluorescence-labeled compounds between neighboring cells[143,145]
9. Dynamic behavior and cooperativity of enzyme clusters (Dynamic Phase Microscopy)[64,135]
10. Measurement of the activation of gene expression associated with a given promoter (by promoter-controlled expression of the luciferase gene or the GFP moiety)[87,147-149]
11. Molecular distances (FRET)[150]

The references given are to be understood as examples only.

Considerable progress has also been made in increasing the resolution in the vertical or z-axis (optical sectioning). While classical differential interference contrast (DIC) microscopy allows resolutions down to 300 nm, this can be increased by video-enhancement (VEC-DIC) to 150 nm or better.[4,5] Also, the digitized images can be subjected to advanced 3D reconstruction algorithms that process full gray-tone images.[5] In the case of fluorescence microscopy the depth resolution is

relatively poor (a few micrometers). This can be improved to a resolution of about 0.7 µm by confocal light microscopy.[6,7] Although in confocal microscopy similar image processing routines are used, this technique will not be covered in detail.

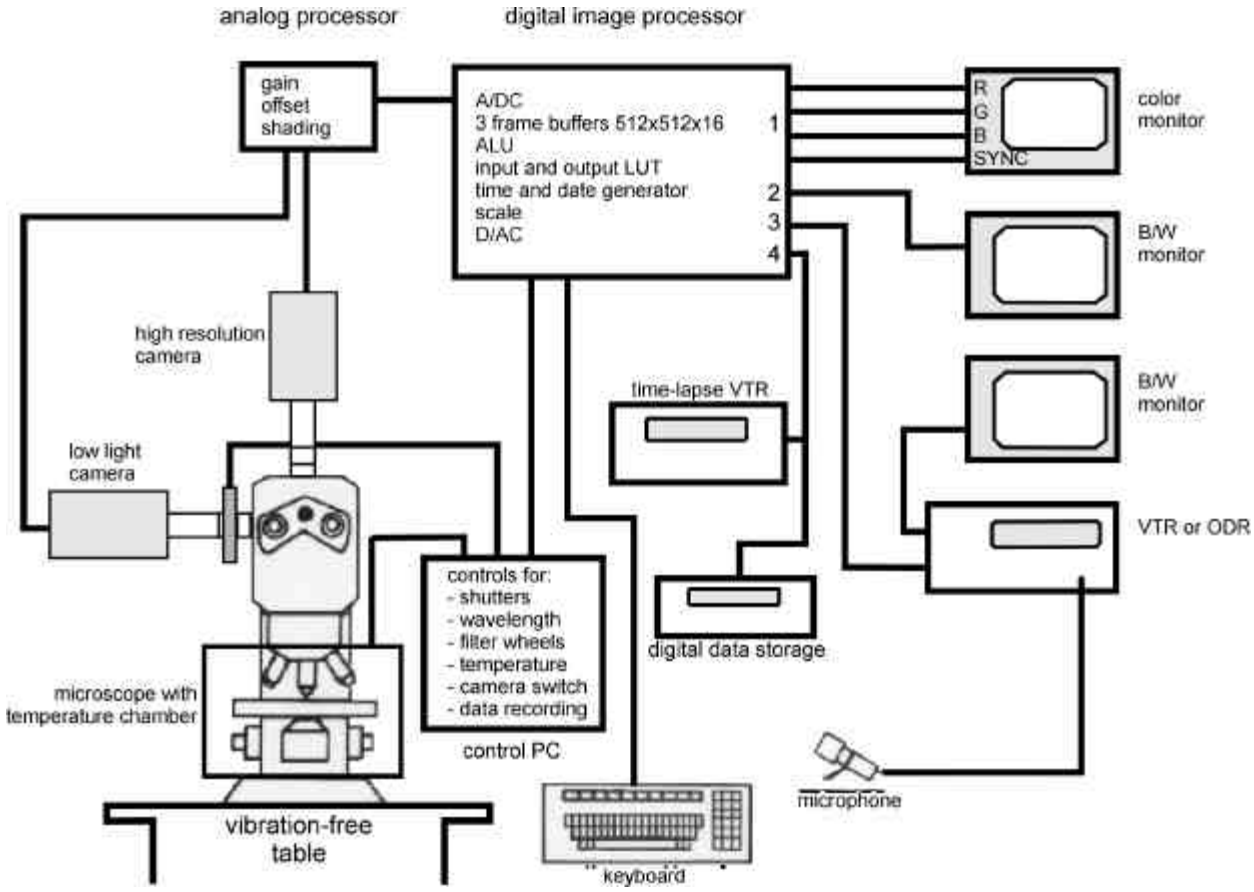

FIGURE 1. Digital light microscopy setup showing the two-stage image processor and the periphery required. Color monitor, raw image monitor and time lapse recorder are not essential but are very useful. VTR, video tape recorder; ODR, optical disk recorder or other high capacity digital storage medium; 1, pseudocolor processed image; 2, raw image for focusing; 3,4, processed image B/W; A/DC, analog to digital converter; ALU, arithmetic logic unit; LUT, look up table; D/AC, digital to analog converter.

II. TECHNIQUES AND THE EQUIPMENT REQUIRED

A. VIDEO-ENHANCED CONTRAST (VEC) MICROSCOPY

A dramatic improvement of image quality is obtained with **video-enhanced contrast (VEC) microscopy**. By increasing contrast and magnification it is possible to extend the limits of both true resolution and visualization and to visualize and analyze in the living state positions and movements of biological objects smaller than 1/10 of the limit of resolution of conventional light microscopy. All membrane-bounded organelles and part of the cytoskeleton can be imaged and their motion and assembly can be studied.[8]

VEC microscopy[4,9-11] and especially the type introduced by R.D. Allen (AVEC microscopy) [11-14] should be applied when finest details are to be visualized with bright-field, differential interference contrast (DIC), or polarization optics. The required procedures are described by Allen et al. and Weiss et al.[10,11,14,15] A schematic representation of the equipment needed is shown in Figure 1. As a result resolution of objects of about 150 nm and visualization of even smaller biological objects such as endoplasmic reticulum[16-21] (Figure 2 and 3 b), vesicles[22,23] (Figure 3 a, c), actin bundles[18-20,24] (Figure 3 a), and microtubules[3,8,13,22] (Figure 3 e to h), down to 20 nm is achieved with visible light in situations where the limit of resolution of conventional microscopy was about 250nm.[4,10,25] Individual colloidal gold particles which are used as tags for proteins can directly be visualized in the 5-10 nm range[26] in theory even down to 1-3 nm.[25,27]

In VEC microscopy the resolution is increased by a factor of almost 2 and the visualization of small objects by a factor of 10, provided that optimal optics are used. This is due to the fact that optics with the highest working numerical aperture can be used at full aperture settings, that the resulting excessive image brightness due to straylight can be suppressed electronically by an offset voltage, and that for electronic imaging devices Rayleigh's criterion of the limit of resolution is replaced by the more advantageous Sparrow criterion.[4,10] According to Rayleigh's criterion two objects appear as resolved, i.e., as separated for the average human observer, when the depression or “trough” in the summed intensity distribution measured across the objects’ Airy disks is at least 15% of the the objects intensity. Using the Sparrow criterion the objects may be closer together so that the intensity distribution between them may almost approach a horizontal line, because almost infinitely small intensity changes can be enhanced to visible contrast with electronic means.[4,10] However, subresolution objects are not imaged themselves but as their much larger diffraction patterns, so that very small objects appear inflated by diffraction up to the size of the resolution limit. Given a separation of more than 200 nm from neigboring structures, such objects can be clearly seen and their position and movements can be determined to nanometer accuracy.[3,22,28-30]

1. Equipment

When working at extremely high magnifications as is possible with VEC microscopy the microscope requires modifications to allow the use of the technique to its full extent.[4,10] A stabilized microscope stand, a very bright illumination system and an oil immersion condenser (both NA 1.3 or better) are recommended.[4,10] Additional magnification changers for optical magnification of 2x or 4x in addition to a 100x oil immersion objective have to be installed to reach the necessary magnification on the TV monitor of up to x10,000 (at a screen width of 25 cm). Image transfer to the camera should preferably be by direct projection onto the camera target and involve as few lens elements as possible. For polarized light techniques a de Sénarmont compensator setting is recommended (see *step 4* below).[10,12,13]

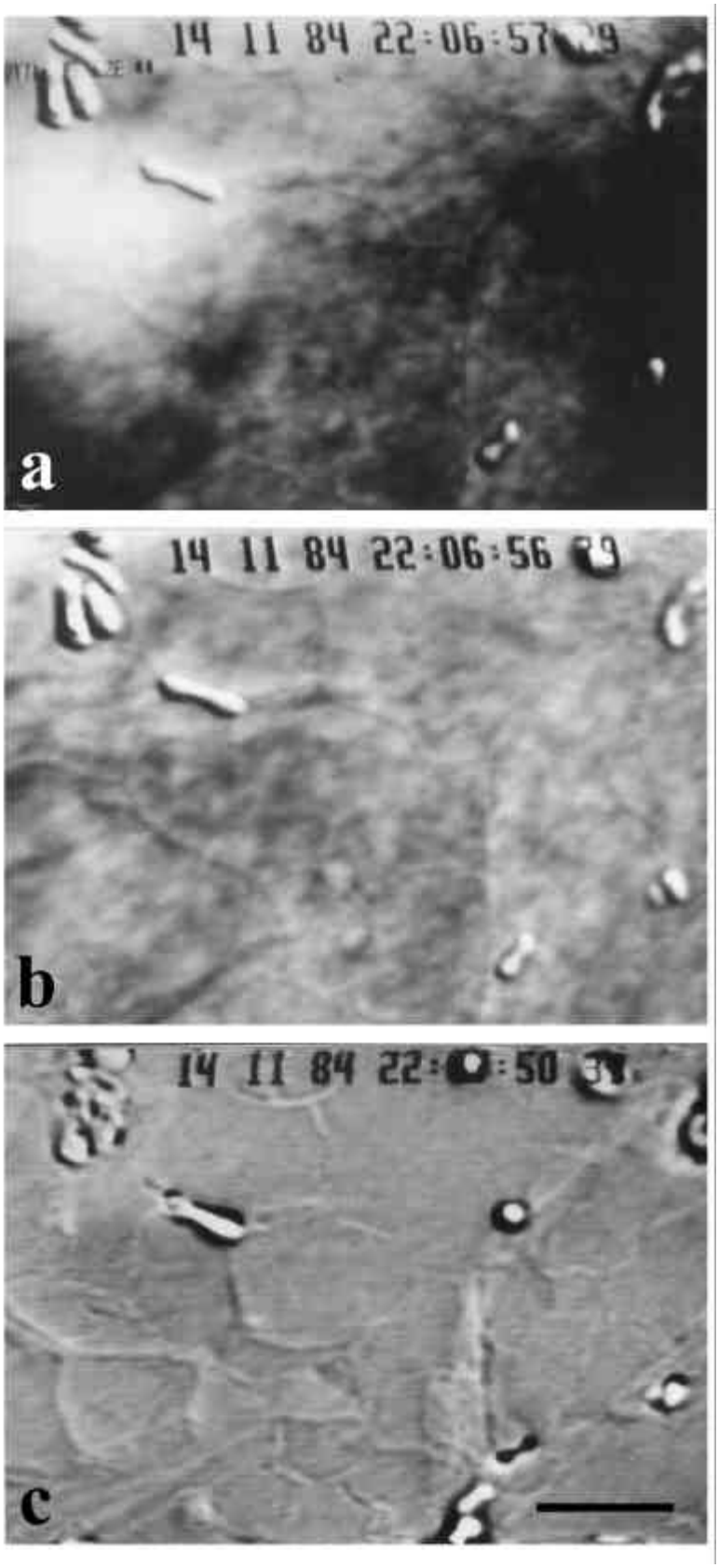

FIGURE 2. Visualization of sub-resolution structures by image processing. The specimen is a plant epithelial cell. (a) Analog contrast enhancement of the microscopic image brings about more image detail but also enhances unevenness of illumination and sometimes a disturbing mottle pattern. (b) A "cleaned" image is obtained after subtraction of the background pattern. Storing and subtracting an out-of-focus frame and then applying digital contrast enhancement brings about subresolution endoplasmic reticulum and cell wall structures. (c) Sometimes static objects such as cell wall fibers become so prominent after contrast enhancement that small details of interest in the cytoplasm in the same focal plane cannot be seen. However, if the image in (a) is stored in the frame memory while still in focus, and then subtracted as “fixed pattern noise” from the consecutive incoming video frames, a picture containing only the moving cytoplasmic elements is derived (differential image). The thin, tubular endoplasmic reticulum can be observed in this way to form a motile polygonal network that would have remained invisible otherwise.[18] Bar 5 µm.

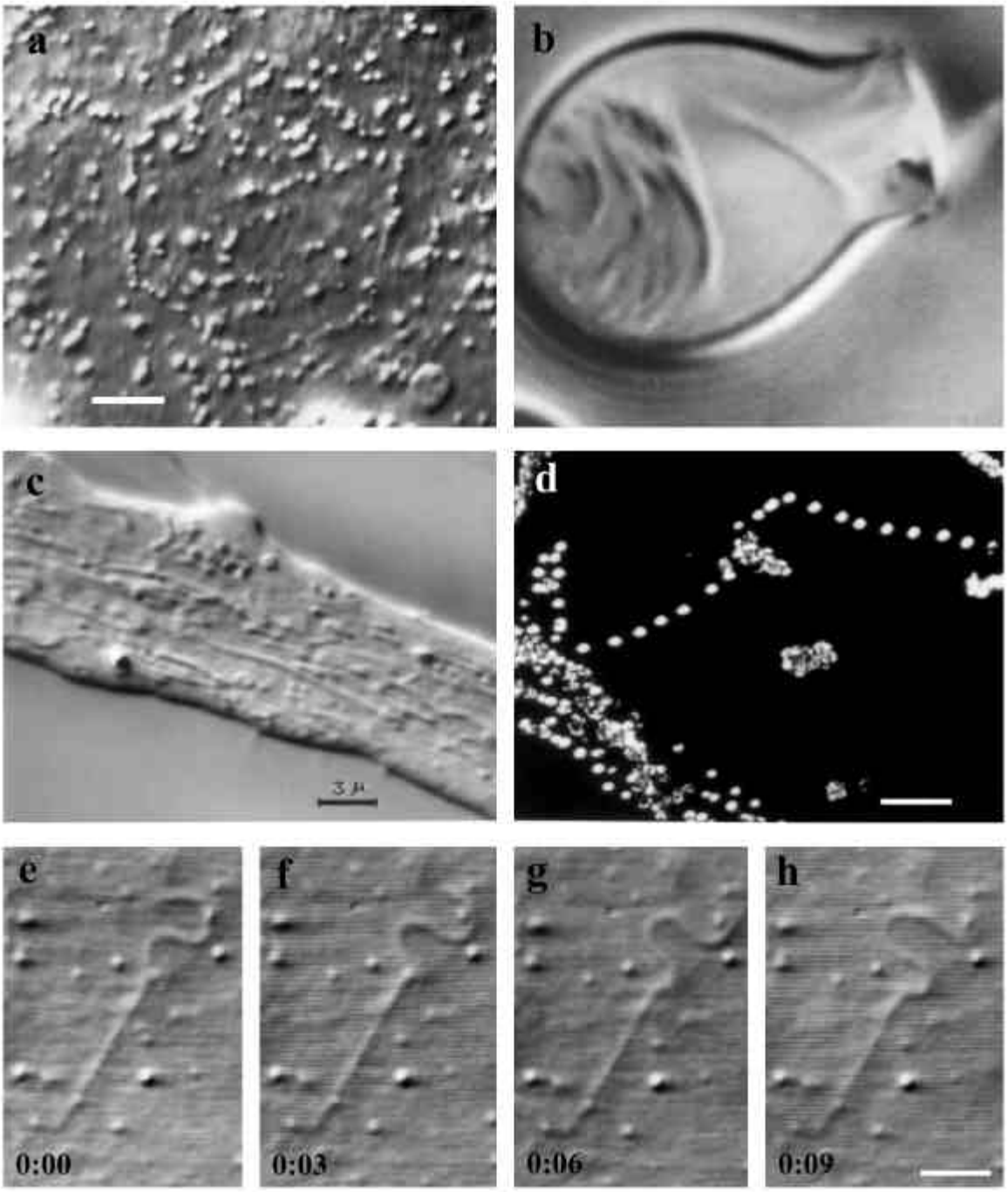

FIGURE 3. Examples of applications of AVEC-DIC microscopy. (a) A rotating hexagon consisting of a microfilament bundle forms in a drop of extruded cytoplasm of *Nitella*. Bar 5 µm. (b) Isolated nematocyte of *Hydra* which can be stimulated to explosively eject its tubular contents. Bar 2 µm. (Courtesy of T.Holstein and W.Maile.) (c) Neurite of a N18 neuroblastoma cell in culture. Most of the organelles move either anterogradely or retrogradely with velocities of 0.5-2 µm/s. The smallest objects are synaptic or similarly-sized membrane precursor vesicles (From Weiss, D.G., in *Recent Advances in Neurocytochemical Methods*. Calas, A., Ed., Springer-Verlag, Berlin 1991. With permission.) (d) Organelle motion made visible by adding differential images as in figure 2c to a frame memory in 1 second intervals ("trace" function of the Hamamatsu Photonic Microscope System). Organelles are spherosomes moving along actin filaments in a plant cell. Actively transported organelles form traces while particles in Brownian motion (center) show a clearly different pattern. Bar 5 µm. (a.-d) Objective lens, 100x planapochromat, NA 1.3; additional optical magnification, 2-4x; microscope, Polyvar Met, Reichert (Vienna, Austria); processor, Hamamatsu Photonic Microscopy System with Chalnicon camera. (e.-h) Native microtubule (diameter 25 nm) from extruded squid giant axon undergoing fishtailing motion.[22,57] Zeiss Axiomat, 100x planapochromat, NA 1.30, oil; additional optical magnification, 4x; 50 W mercury lamp; processor, Hamamatsu Photonic Microscopy System with Chalnicon camera; sequence, 9 seconds; bar, 1.5 µm.

For VEC microscopy a geometrically distortion-free, high resolution video camera (Chalnicon, Newvicon or Pasecon) or a high precision CCD (charge-coupled device) camera is required. The cameras must have externally adjustable offset (black level) and gain to allow for analog contrast enhancement.[4,8,10,12,13] Automatic gain control (AGC), if present, must be disabled.

For most applications it is very important that the image processing equipment contains a unit for **analog** contrast enhancement of the analog video signal (Figure 1). Applying analog contrast enhancement by manually setting gain and offset one yields a high contrast image even for very low contrast or low light objects. Only such enhanced images should then be digitized (at a resolution of at least 512x512 picture elements (pixels) with 256 gray levels) and subjected to arithmetic operations in the frame memory of a **digital** real time processor (Figure 1). For VEC microscopy one needs digital frame averaging to remove pixel noise, continuous digital background subtraction to remove unwanted fixed pattern noise (mottle)[10,14] (Figure 2 b) or, if required, non-moving image details[18] (Figure 2 c). Digital contrast enhancement (stretching of the gray level histogram) is another essential function usually required after image subtraction. For the dual wavelength fluorescence ratio imaging techniques (e.g., Ca^{2+} imaging with FURA2 [31,32,33]) the image processor must have the additional capability of fast division of full video frames. Digital microscopy as discussed here involves the processing of full gray-level images at video frequency (40 ms), so that we need **real-time image processors**.[10,14,34] More technical details on the equipment required are published elsewhere.[4,10,34]

Video-microscopic images which have been created by real time image processing, can be subjected to classical image analysis in order to obtain information on morphometric parameters. This is done after thresholding, i.e. with binary images (usually not in real-time) and it will require conventional **image analysis systems**.[35,36]

2. Sample Preparation

Basically the same samples and the same contrast techniques as for conventional light microscopy can be used in VEC microscopy. The specimen's region to be studied should be close to the cover glass surface, where the best image is obtained. If the highest magnifications are intended, Köhler illumination may only be achieved at the surface and a few tens of micrometers below (upright microscope), since high magnification objectives are usually designed for optical imaging of objects at a distance of 170 µm from the front element. Note that spherical aberation will be introduced since the oil-immersion objective will be focussing partially through water rather than glass. Alternatively for imaging deep within aqueous specimens, a water immersion objective may be employed to overcome the problem. If thicker specimen, such as tissue slices, vibratome sections or nerve bundles are to be observed, only DIC or anaxial illumination[37] techniques are recommended. The opacity of living tissue can be greatly reduced when infrared or near infrared (IR) light is used.[38]

3. Image Generation and Improvement

Allen et al.[12,13] and Inoué[39] simultaneously described procedures of video contrast enhancement for polarized-light techniques. Allen named his techniques "Allen video-enhanced contrast" differential interference contrast and polarization (AVEC-DIC and AVEC-POL respectively) microscopy. The AVEC techniques involve the introduction of additional bias retardation by setting polarizer and analyzer relatively far away from extinction. Allen recommended a bias retardation of 1/9 of a wavelength (20° away from extinction as the best compromise between

high signal and minimal diffraction anomaly of the Airy pattern.[12, 40] This setting has the best signal-to-noise ratio and resolution, but its use was prevented because the image is much too bright for observation by eye due to the enormous amount of stray light introduced at such settings. This can, however, be removed by an appropriately large setting of analog and/or digital offset. The steps required for image generation and improvement for the highest resolution and for visualization of sub-resolution objects by VEC microscopy include procedures different from those used in conventional microscopy. The best results are obtainable with the procedure described below for AVEC-DIC. However, if DIC is not required, such as for bright-field, dark-field, anaxial illumination, Hoffman contrast or fluorescence microscopy, step 3 should simply be omitted. A more detailed description, including some theory and more technical hints, is given elsewhere.[10]

Step 1. Focus the specimen. If the entire specimen consists of invisible, sub-resolution size material (density gradient fractions, microtubule suspensions, unstained EM sections) it will be difficult to find the specimen plane. It may help, if you apply a fingerprint to one corner of the specimen side of the cover glass and use the oil droplets for focusing.

Step 2. Adjust Köhler illumination. It is important to make sure that the camera receives the proper amount of light to work near saturation. Since we will apply extreme contrast enhancement later, we have to start out with as even an illumination setting as possible. Proper centering of the lamp and setting of the collector lens are therefore essential.

Step 3. Open the condensor diaphragm fully in order to utilize the highest possible numerical aperture to obtain highest resolution. Any iris diaphragm of the objective should be fully opened. Be careful to protect the camera from high light intensity prior to this step. This setting will result in a small depth of focus, especially with DIC (optical sections of 0.3 µm or less with 100x oil objectives).

Step 4. (Only for polarized light techniques). Set the polarizer (AVEC-POL) or the main prism or compensator (AVEC-DIC) to 1/9 of a wavelength (20° off extinction).[10,11] The optical image, that is that seen in the oculars, will disappear due to excessive straylight. The illumination may have to be reduced to protect the camera using neutral density gray filters (but not by closing condenser or objective diaphragms). At this point one has to ensure that the camera still receives the proper amount of light to work near its saturation. Some manufacturers have red and green LEDs built in to indicate the illumination situation. One should see a moderately modulated image on the monitor, while a *very* flat or no image indicates insufficient light.

Step 5. Analog enhancement. Increase the gain on the camera to obtain good contrast. Then apply offset (pedestal). Always stop before parts of the image become too dark or too bright. Repeat this procedure several times, if necessary. Make sure that the monitor for watching the changes is not set to extreme contrast or brightness. Analog enhancement improves the contrast of the specimen but unfortunately also emphasizes dust particles, uneven illumination and optical imperfections. These artefacts, called "mottle", are superimposed on the image of the specimen and may in some cases totally obscure it. Disturbing contributions from fixed pattern noise (mottle) or excessive amounts in unevenness of illumination can be tolerated if digital enhancement is performed later (*step 7*).

Step 6. Move the specimen laterally out of the field of view or (when using DIC) defocus it (preferably towards the cover glass) until it just disappears. The result is an image containing

only the imperfections of your microscope system as fixed pattern noise (background mottle pattern).

Step 7. Subtract background. Store (freeze) the mottle image in a digital frame memory, preferably averaged over 8 to 64 frames, and subtract it from all incoming video frames. You should see an absolutely even and clean image, which may, however, be weak in contrast. If motile organelles need to be visualized free of immotile in focus background objects (fixed pattern noise), an in focus background image has to be subtracted (Figure 2).

Step 8. Perform digital enhancement. This is done by alternating between stretching a selected range of gray levels and shifting the image obtained up and down the scale of gray levels until the optimal result is found. Displaying the gray level histogram will be helpful to select the upper and lower limits of the image information, which have to be defined as bright white and saturated black respectively. If the image is noisy (pixel noise) go to step 9 or 10.

Step 9. Use an averaging function in a rolling (recursive filtering) or jumping mode over 2 or 4 frames. This will allow the observation of movements in your specimen, but very fast motions and noise due to pixel fluctuations will be averaged out. Averaging over longer periods of time will filter out all undesired motion such as for example distracting Brownian motion of small particles in suspension.

Step 10. If needed, apply additional digital procedures for spatial filtering to reduce noise, to enhance edges of objects or to reduce shading.[35, 41,42]

4. Interpretation

Unlike in EM images, which truly resolve the submicroscopic objects depicted, the sizes of subresolution objects seen by VEC-microscopy may not necessarily reflect their real size. Objects smaller than the limit of resolution (180 - 250 nm, depending on the optics and the wavelength of light used) are inflated by diffraction to the size of the resolution limit (e.g., Figures 3 e to h). Whereas the size of the image does not enable a decision on whether one or several objects of a size smaller than the limit of resolution are present, the contrast sometimes permits such a judgement. A pair of microtubules would, for example, have the same thickness as a single one, but the contrast would be about twice as high. If large numbers of sub-resolution objects are separated by distances of less than 200 nm from each other (e.g. vesicles in a synapse), they will remain invisible, but they will be clearly depicted if they are separated by more than the resolution limit. Also remember that, if in-focus-subtraction (Figures 2c and 3d) or averaging are used, the immobile or the moving parts of the specimen, respectively, may have been completely removed from the image.

B. VIDEO-INTENSIFIED MICROSCOPY (VIM)

Low-light video-microscopic techniques aimed at the visualization and quantitation of weak monochromatic images obtained by fluorescence microscopy are called **video-intensified microscopy (VIM)**. Fluorescence microscopy images are two-dimensional arrays of fluorescence measurements that contain information on the amounts and distribution of intracellular metabolites, dyes, antigens, or exogenously added fluorescent probes. Typical parameters for VIM measurements include Ca^{2+}-concentration, pH value, metabolites, and membrane potential as determined by the use of specifically developed fluorescence indicator dyes, or the distribution

of fluorescence-labeled antibodies. Specific, non-toxic fluorescent dyes are available to verify the biochemical identity of the cellular structures seen by conventional or video-microscopic techniques.[43-45]

1. Equipment

When video-rate observations are required for the detection of dynamic changes in real time in illumination situations at the limit of human vision or below, a low light level camera such as a one or two stage silicon-intensifier target (SIT or ISIT) camera or a microchannel plate-intensified device is required.[4,10,34, 46] However, due to signal noise high sensitivity and high spatial resolution tend to be mutually exclusive features of these cameras. In contrast, cooled slow-scan CCD cameras provide high sensitivity while maintaining a high spatial resolution. To ensure this, images must be recorded at a slower rate. Photon-counting cameras are required when extremely weak signals, i.e. luminescence or autofluorescence need to be imaged at illumination conditions up to six orders of magnitude below the threshold of human vision or of photographic film.[6,10] Microscope setups similar to those shown in Figure 1 for VEC microscopy are also suitable here. The technical specifications of low light level cameras and further information on the procedures and equipment needed have been described in more detail elsewhere.[4,10, 46]

2. Image Generation

Most high-resolution cooled CCD cameras will record images with a dynamic range of 12bit (4096 gray levels) instead of 8bit (256 gray levels) used by most regular digital light microscopy systems. The high dynamic range of these cameras makes them especially suitable to record fluorescence images. One should, however, be aware that most image processing software packages such as PhotoShop (Adobe Systems, Inc., San Jose CA, USA) or Paint Shop Pro (Jasc Software, Inc., Minnetonka MN, USA,) can only handle 8bit gray level and 24bit color images. From advances in computer technology more sophisticated software can be expected in the near future that will be able to handle 12bit gray and 36bit color images. Keeping in mind the limitation of the current image processing software, particular care should be taken when choosing the proper exposure time. It is recommended to take several images at different exposure times.

Using cooled CCD cameras multi-color fluorescence images can be generated from specimens stained with multiple fluorescent dyes. In this case the correct exposure of the individual images is particularly important. First, single images for each fluorescent signal are generated. It should be noted here that the original images should always be saved uncompressed and in a file format which is universally accessible by the various types of image processing software (e.g., .tif). The individual images are then saved as 8bit B/W images in .tif file format. Color images are then composed in e.g. PhotoShop (Adobe Systems, Inc.) or similar programs using the 24bit RGB option of the software. Before generating a color image the intensity range and the level of all images to be merged should be adjusted, so that the whole range of intensities available for that color is used (24bit for all three colors). The color image can then be generated by opening a new image file of appropriate size (matching that of the images to be merged) in the RGB mode and copying the single B/W images in either one of the red, green, and blue image layers.

C. MOTION ANALYSIS

Since the advent of digital light microscopy allowed the visualization of all cell organelles and some cytoskeletal elements in their vivid dynamics, the desire to analyze the cytoplasmic motion arose.[47, 48] Methods to quantitatively describe intracellular motility by a large number of parameters such as velocity, straightness of path, length of excursions, reversals of direction, pauses, and others are now in use.

1. Equipment

Software-based systems working in conjunction with modern frame grabber boards are capable of multiple object tracking. Usually these devices detect objects whose brightness is above an adjustable threshold, and which are located in an adjustable region of interest. More advanced systems include object parameters such as size, shape, or color to select the objects to be analyzed. Superimposed cross-hairs indicating the centers of the objects and their vertical and horizontal diameters follow automatically if the objects move. The positional coordinates are continuously collected at video frequency (1/25 or 1/30 sec depending on the video standard used). The MaxVideo system (Datacube, Inc., Peabody MA, USA) combined with the Area Parameter Accelerator board (APA512-MX, Vision Systems, Adelaide, Australia) does provide such a system.[49,50] This combination was one of the first capable of describing each object by a set of up to nine basic descriptive parameters (e.g. number of pixels, perimeter, minimum and maximum x and y coordinates etc.). Connected regions of either black or white pixels are recognized as objects. A set of parameters for all detected objects is compiled in a list for each video frame at video frequency. From a sequence of such particle parameter lists the multiple trajectories can be derived by nearest neighbor analysis.[49]

More recently PC-based systems which are designed as part of video-microscopic workstations became available, e.g., MetaMorph (Universal Imaging Corp., West Chester PA, USA) or MicroTrack (HaSoTec GmbH, Rostock, Germany). Many procedures for motion analysis are based on classical time series analysis and are, therefore, similar for cell organelles, single cells, microorganisms and laboratory test animals. Additional software packages designed for applications with whole organisms and for environmental or pharmacological testing, as well systems for the analysis of sperm motility can, therefore, often be used with good results[51] (see also other chapters in this volume). Problems may, however, arise when fluorescent organelles detected by VIM are to be tracked, because of their often noisy appearance and sometimes ill-defined margins. A special system for the analysis of green-fluorescent protein-(GFP)-labeled organelles was recently described, that uses fuzzy-logic algorithms for object detection.[52]

2. Tracks and Trajectories

In order to learn more about the type of motion the time series of the individual organelle coordinates is to be analyzed. For both, recovering information on the tracks and on the specific type of motion it is necessary to obtain first the trajectory data.

The features of the MicroTrack program may serve as a typical example (Figures 4 and 5). First one defines the conditions for recognition of the desired particles: brightness of the particles (the light intensity of the objects can be above or below the gray level of the background, in Figure 4 the bright particles have been selected), size limits (maximum and minimum area in pixels) and form characteristics (roundness, minimum and maximum width and height, etc). The detection of

particles is performed within a user-defined region of interest (ROI). Also additional experimental and control regions can be defined. For each experimental region a maximum number of objects to be tracked can be defined. The data for all recognized objects are then saved to the hard disk and can be analysed, exported and printed later. Data for each second video frame are extracted online or during playback from tape. It is useful to have a summary screen that shows the accumulating positions of all recognized particles (at the right hand side). Connecting the consecutive positional data points of the moving objects by software yields the trajectories (Figure 5). The example given, protoplasmic streaming of organelles in an onion epithelial cell, clearly shows regions of directed motion (center), regions of stochastic motion (top and below), and regions without moving particles.

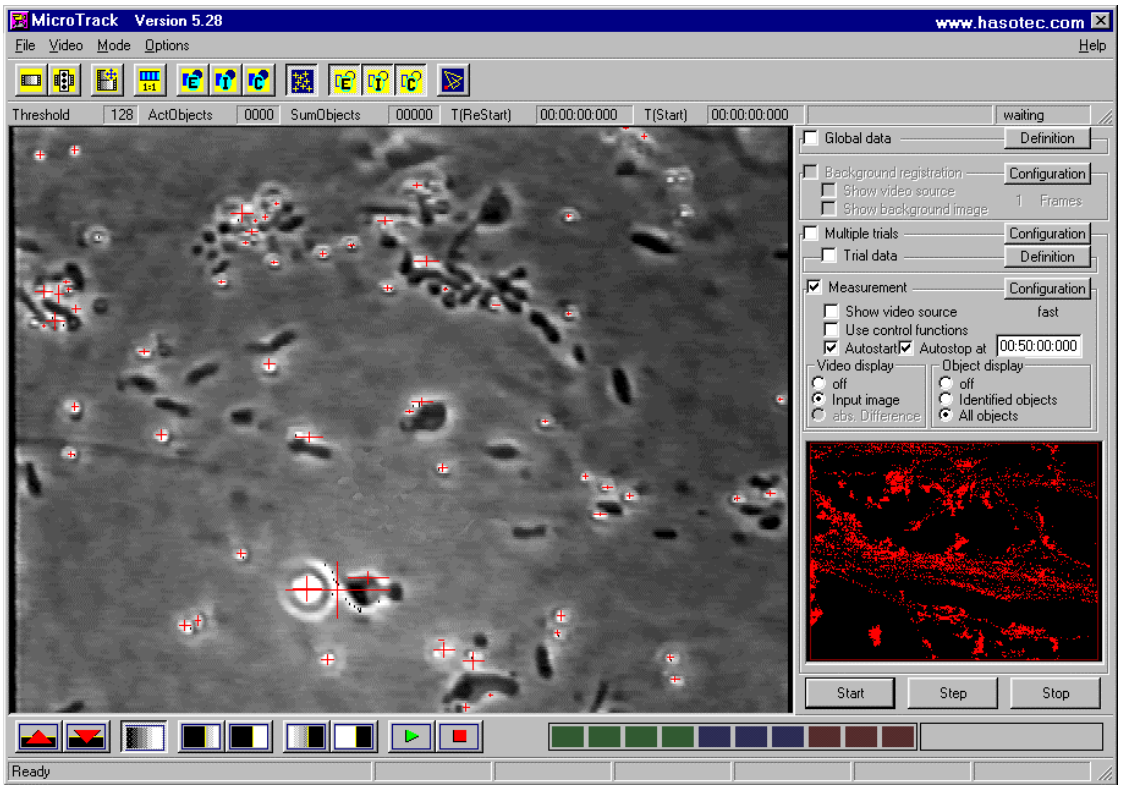

FIGURE 4. Detection of moving organelles. Screen shot of the MicroTrack motion analysis system during an online measurement (analysis screen) of protoplasmic streaming in a plant cell. Loading and saving data files is performed within defined regions of interest (here entire screen). Each second video frame is being analysed online in this example. Dimensions of all ojects matching the selected criteria are marked online by crossbars. The summary screen (right hand side) shows the accumulating data of the movements of all recognized particles. Frame grabber, FG32Path; software, MicroTrack 5.28 (both from HaSoTec GmbH, Rostock, Germany); width of the digitized image displayed, 28 µm.

In VEC-DIC microscopy of whole cells the moving objects and the underlying track (microtubule or microfilament) cannot be seen simultaneously. If its position in the cell has to be described we have to estimate the track by fitting a curve to the observed x,y-positions of the object. Visualization of microtubules revealed that the majority of them forms straight tracks and that their diameter is small compared to the size of the organelles being transported.[53] This holds true for microtubules in axons, as well as for free microtubules. Estimating the track is hence reduced to fitting a straight line to the observed positional data of the particle. One has, however, to consider that the commonly used regression model to fit a curve is not appropriate in this case because it assumes that y-values are measured with random errors, while x-values are without errors so that the estimation of the regression curve minimizes the sum of the squares of the

distances of the measured y-value and the y-value of the curve. In our case, however, both, the x- and the y-values are subject to measurement errors. Therefore, the sum of squares of the perpendicular distances of the x,y-positions to the line (track) has to be minimized.

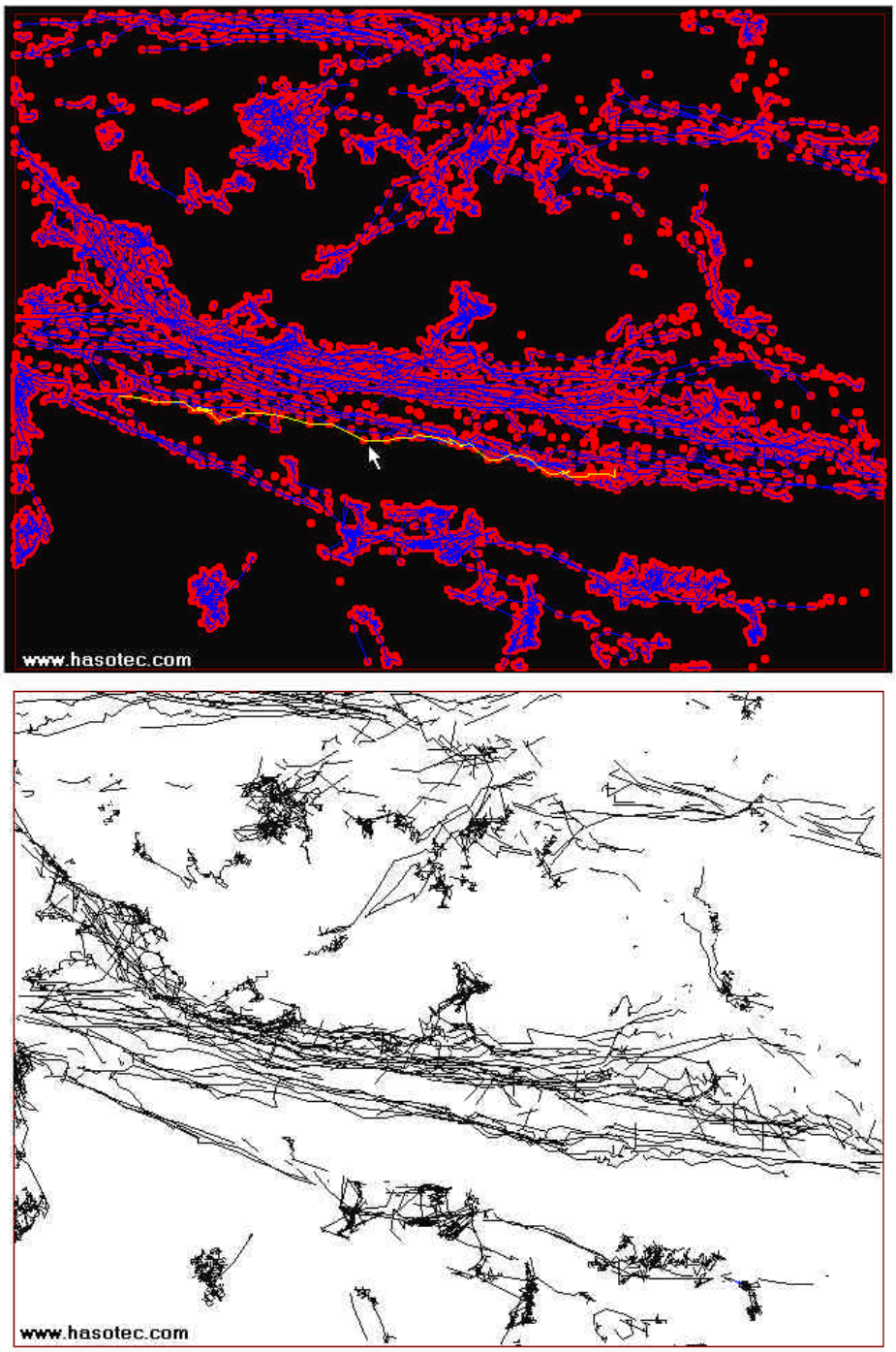

FIGURE 5. Generation of trajectories of moving organelles. (a) The dots show the accumulated positions of the centers of mass of the objects using a constant scale factor and the lines represent the trajectories of the respective particles. The track marked by arrowheads is further analyzed (see Figure 6). (b) Cumulative trajectory raw data provide a good overview of the intracellular position of tracks for the movement and of regions of Brownian motion (top and below).

The slope a and offset b of the fitted line g(x)= y = a x + b are given by equations

(1) $a^2 S_{xy} + a(S^2_x - S^2_y) - S_{xy} = 0$ and

(2) $y = ax + b$

where S^2_x, S^2_y and S_{xy} are the variances and the covariance, and *y* and *x* are the means of the x- and y-values. For a more detailed explanation and the discussion of confidence intervals for the estimated parameters refer to Wong[54] Solving the above equations we obtain an estimate for the track.

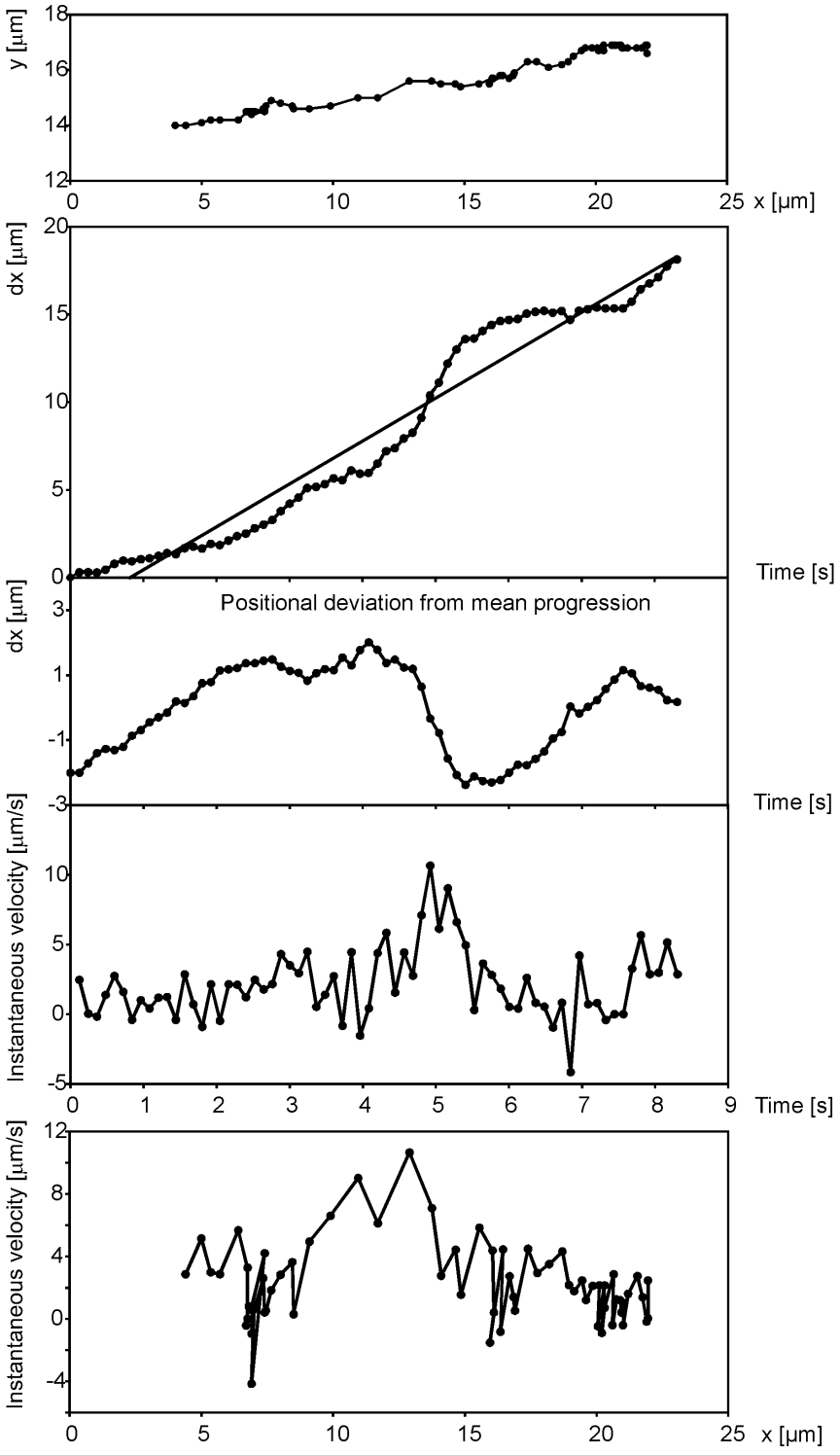

FIGURE 6. Steps of the motion analysis of a moving organelle. (a) Path of the organelle moving toward the right hand side on the video screen. Coordinates measured from top left corner. The movement is a combination of linear motion and pauses with more stochastic motion. (b) Progression of the organelle from start in the main direction of movement plotted versus time. The slope along the curve indicates the instantaneous velocity. The regression line represents the average velocity which is subtracted (trend removal) to yield the positional deviation from mean progression needed further analysis (c). (d) Instantaneous velocity calculated from the progression between two measured time points divided by time and plotted versus time. (e) Instantaneous velocity is plotted versus position in the main direction of movement.[cf. 49,50]

For any observed position of the particle the point of intersection of the perpendicular with the line yields its estimated position on the track. If we transform the coordinate system in a way, that the origin is translated to the estimated starting position of the particle on the track and the x-axis is rotated onto the estimated line (track), we obtain the desired horizontal representation of the trajectory for further motion analysis. The resulting equations for the translocation and rotation were given by Weiss et al.[49] The motion of the particle is now described by two time series, one representing its position on the track (x-direction) and the other its perpendicular deviation (y-direction).

3. Motion Analysis

The analysis of the motions is usually based on time series analysis similar to the procedures described by Koles et al.[55,56] and performed either with one of the above-mentioned motion analysis software packages or, alternatively, with commercial calculation programs (e.g., Microsoft Excel) or statistics and mathematics program packages which allow the programming of macros such as those developed in our laboratory.[49,50,57]

One very useful parameter to describe the motion of an organelle in more detail is the average velocity in the major direction of movement. This can be calculated in different ways, e.g. as the slope of the line fitted to the positional data over time, as the average of frame to frame velocities, or as the ratio of distance and time for the whole tracked path. The latter method is used in our work.

If the molecular mechanisms of the intracellular transport are studied, the analysis of time- and track-dependent variations of the velocity in a single trajectory are of interest, because they can give insight into the mechanism of action of the underlying motor enzymes. In contrast to the average velocity this is called 'instantaneous' velocity. The methods to obtain the estimate of the instantaneous velocity vary,[55,58] so that we describe our approach in more detail. Some difficulties will emerge when the velocity is estimated from the positional data since the coordinates are likely to be affected with measurement errors. The velocity of a particle is obtained by differentiation of the time series of x-positions. First-order differencing according to

$$v(t) = (x(t) - x(t-1))/\Delta t, \quad (3)$$

where Δt is the time between successive x-positions, is generally considered to be a rather gross approximation to differentiation. We decided, however, to use this method for the following reasons for our studies on the existence of low frequency velocity oscillations as claimed by Koles et al.,[55,56]. Due to our sampling frequencies (2 Hz to 25 Hz) the maximum resolvable frequencies of the positional variation of a particle are then 1 Hz to 12.5 Hz. In nearly all observed spectra more than 99% of the power of the signal is well below 1 Hz. Obviously the signal is 'oversampled' and we therefore obtain, with respect to the signal, a 'small' t and hence a better approximation to differentiation. Noise components at higher frequencies, induced by measurement errors, would, however, still degrade the estimate severely, because high frequency components are 'amplified' by differentiation. Therefore, we remove critical noise components at higher frequencies, before differencing the time series according to (3) in the following way.

First, the average velocity of the particle (trend) that is represented by the regression line is subtracted from the data set (see Figure 6 b and c). Then, we transform the trend-removed time series of the x-positions into the frequency domain, using the Cooley-Tukey fast Fourier transform (FFT) algorithm.[59] Second, a cut-off frequency for low-pass filtering, usually in the

range of 0.3 to 0.7 Hz, is determined from this spectrum. Third, the trend-removed time series is digitally filtered using a low-pass filter (second order Butterworth seemed appropriate) with the respective cut-off frequency. Fourth, the trend is re-added to the filtered time series. After differencing, according to (3), we finally obtain the particle's instantaneous velocity, which is plotted versus time and versus the main direction of movement. This data set is now well suited for a spectral analysis by FFT analysis to determine, whether the motion contains regularities in position or velocity, such as oscillations or jumps, or whether it is continuous with added stochastic fluctuations.[29,30,49] We found that the velocity fluctuations observed in axons are stochastic and that the regular velocity oscillations described by Koles et al.[55,56] seem to be sampling artifacts.[49]

If movement episodes are short, e.g. for very fast movements in plant cells, the data sets are not suitable for filtering and FFT analyses and have to be plotted as raw data as shown in Figure 6 for a single organelle. Most of the parameters characterizing the movement can also be averaged for a group of particles.

D. DYNAMIC PHASE MICROSCOPY

Our eyes react to spatial intensity distributions within a limited range of wavelengths and an image is then associated with the real object by intellectual processes. However, using modern, computer-aided electro-optical techniques it is possible to encode and represent on a monitor other physical values or functions of our optical environment which are inaccessible to direct vision, such as e.g. UV, IR, i.e., temperature fields, or the phase information of light. The nature of the chosen physical value and the information available depend on the converters and algorithms used. The thermovision technique, which is now widely used in medicine and other fields is one example of such functional imaging.

In the 80's profilometry was developed as a new branch of optical instrumentation, aimed at a quantitative evaluation of subtle surface structures and roughness. This technique is based on the dependence of the phase of a reflected wave on the distance of the surface from the light source, i.e. the local surface height. The phase is shifted by 2π for each distance equal to the wavelength used, which serves here as a natural length standard. Phase measurements are performed using interferometric methods, i.e. comparisons with the phase of the reference wave. Modern commercial interferometers with coherent laser sources allow to measure extremely small optical path differences (OPD) of 10^{-6} – 10^{-8} of a wavelength so that height differences of few nanometers are detectable. The phase images of surfaces are usually obtained by scanning mode measurements and represented as 2D pseudocolor maps of OPD h(X,Y) in the image plane X,Y. They are similar to geographic maps, however with the height values on the nanometer scale and the X- and Y-distances on the scale of a few micrometers. For solid state objects OPD values correspond to the real height variations. For the complicated, non-uniform structure of living cells the meaning of OPD is less well defined since these values depend on the surface profile *and* the 3D refractive index distribution.

Unstained and transparent biological objects are also phase retarding objects. Phase microscopy of thin biological objects can be based on local measurements of OPD values in reflection mode. Here, refractive index differences of the optically inhomogeneous internal structures of a cell, which is placed on a polished, reflecting surface, dominate the local OPD values and create the image contrast. The sensitivity, i.e. the amount of contrast and resolution, of phase microscopy methods is comparable with VEC microscopy. Some structures, which are hardly seen in bright-

field mode (light amplitude) can be clearly distinguished in phase microscopy due to the method's high sensitivity to local refractive index differences. In contrast to phase contrast and DIC microscopy which use **relative phase differences** to create image contrast, the phase microscopy as discussed here is based on **direct OPD measurements** and yields absolute values without preliminary conversion into an intensity or an enhanced differential contrast image (Figure 7 b,c). Therefore, the measured OPD values are independent of illumination intensity and are normalized to wavelength. However, the measured OPD, h(X,Y), depends on the product of geometrical height (specimen thickness) H(x,y) and local refractive index difference $\Delta n(x,y)$ in the focal plane x,y which cannot be separated from each other easily. Therefore, interpretation of phase images requires some experience.

The fluctuation or rotation of a single isolated macromolecule between two adjacent pixels cannot be recorded as a significant change of OPD, since the very small changes of refractive index accompanying this motion are averaged within the probe volume and are, therefore, recorded as additional noise only. However in the case of synchronous motion of a sufficiently large number of macromolecules their contribution to OPD may be significant and could be detected as specific frequency component if their temporal oscillations are regular and exceed background.

1. Method

The new method of Dynamic Phase Microscopy (DPM)[60,61] results from electronic periodic profile scanning along a scan-line in a phase microscopy image. The local OPD values and profiles are not constant since cells are living objects and their organelles are moving or changing their configuration in time. In order to describe and image the intracellular fluctuations, the digitized OPD data (in units of height) of a temporal series of height profiles along the scan line s (Figure 7 b) are accumulated as a stack ("track diagram", Figure 7 d). Sections through the track-diagram yield records ("registograms") of phase height fluctuations h(X,t) for fixed scan-line points X over time (line r in Figure 7 d and Figure 7 e). After Fourier transform of such time series one obtains the corresponding spectrum of local phase height or apparent object thickness fluctuations. The whole set of such spectra representing a 2D or 3D position versus frequency plot or X,f-plot (spectral pattern) shows with high spatial resolution the location of dominating frequency components along the scan line s.[60,62]

Since cells and their organelles are optically non-uniform anisotropic objects, phase microscopy of biological objects has some peculiarities, which complicate interpretation of the results. There are no simple algorithms, connecting the measured phase $\varphi(X,Y)$ of the diffracted wave to the shape, i.e., geometrical thickness, H(x,y), and the refractive index, $n_i(x,y,z)$, of an object region. The approximated expression for a measured local phase deviation $\Delta\varphi(X,Y)$ due to change of $n_i(x,y,z)$, is

$$\Delta\varphi(X,Y) = 4\pi\, h(X,Y)/\lambda \approx 4\pi\, \Delta n_i(x,y)\, H(x,y)/\lambda \tag{4}$$

where $\Delta n_i(x,y)$ is the local difference of the refractive indices and λ the wavelength. Therefore, the measured phase thickness, h(X,Y), will be essentially lower than its true value, H(x,y), and a small organelle cannot be identified if $\Delta n_i(x,y) << 1$. Typical phase images of a single mitochondrion are shown in Figure 7 b and c).

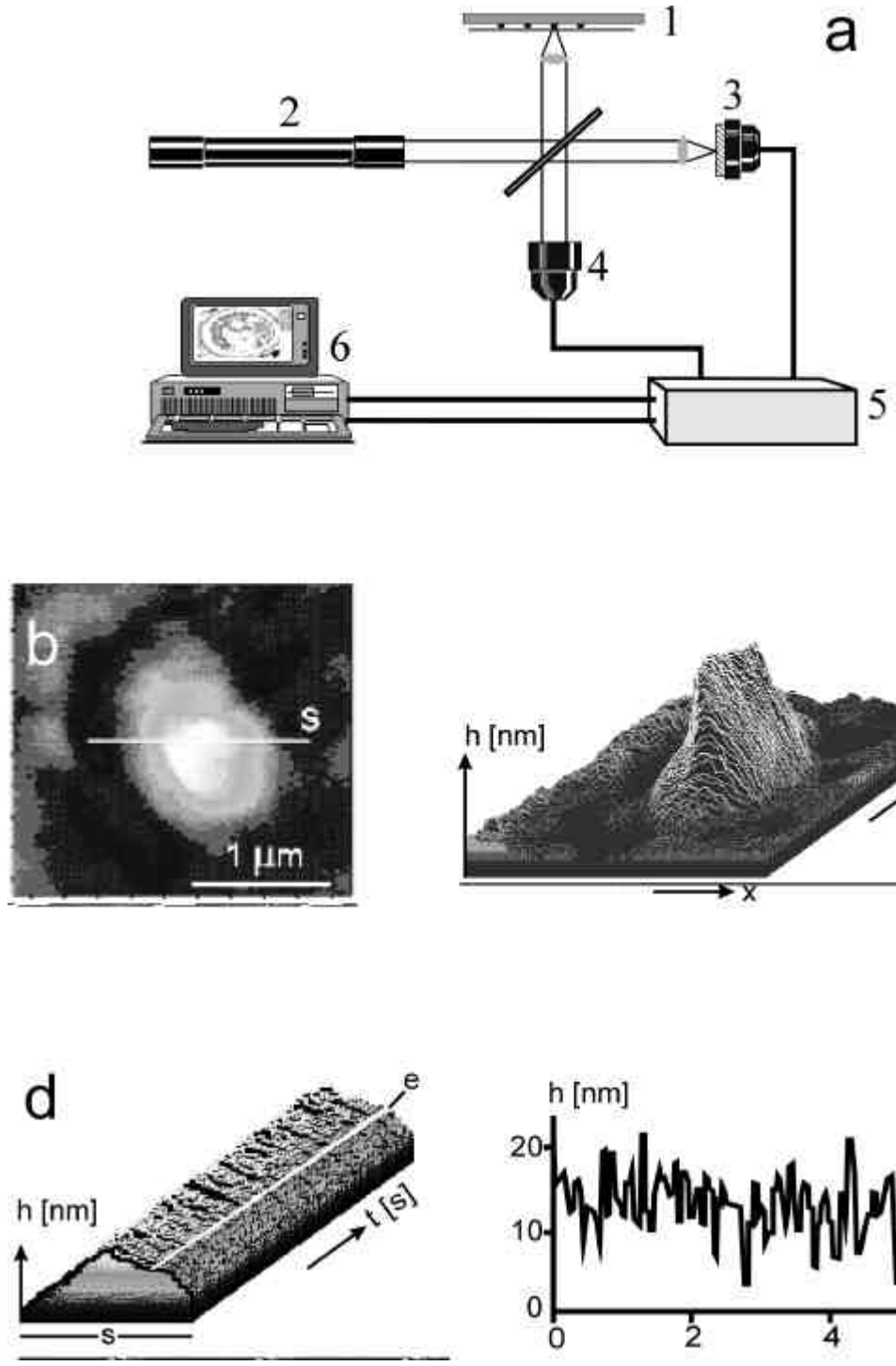

FIGURE 7. (a) Layout of the computer-aided phase microscope "Airyscan" for Dynamic Phase Microscopy. 1, Object on a reflecting surface with cover slip; 2, light from the zero mode He-Ne laser directed onto the beam splitter of the interferometer; 3, reference mirror on piezo-transducer for modulation of the interference pattern; 4, dissector image tube for data collection, 5, control unit; 6, computer. (b) Optical path difference (OPD) image of a single mitochondrion showing local phase hight distribution. S, position of the scan line. (c) 3D-visualization of the phase hight profile in OPD units. (d) A series of phase hight profiles measured along the scan line chosen in (b). Temporal fluctuations of OPD values are obtained for a given point on the scan line s if data are collected over time (line e) (e). If these plots are obtained for all points of the scan line and represented in 3D one obtains the phase hight fluctuation map that can be further subjected to spectral analysis by FFT for obtaining the X,f spectral pattern.

The square of the deviation of measurements of a height standard $I(X) = \sigma^2(X)$ is used for a quantitative evaluation of the intensity of fluctuations. This results in information on the intensity distribution of fluctuations along the scan-line axis X. One uncommon feature of phase images is the super-resolution. For objects with sufficiently high OPD contrast it is possible to exceed the classical resolution limit 4-6 times. The evidence for super-resolution in phase images was first shown using measurements of sub-micron semiconductor structures and latex spheres[62,63] and arguments for its plausible explanation based on photon tunneling were given.[64]

2. Equipment

The Computer Phase Microscope "Airyscan"[65] is an interference microscope according to the Linnik layout (Figure 7 a), with phase modulation of a reference wave. A He-Ne laser is used for coherent illumination of the object and a dissector image tube as a co-ordinate-sensitive photodetector. In this microscope the measurements of thin transparent biological objects located on a polished, reflecting substrate, are performed in reflected light mode. The size of the field of view can be changed from 5 to 50 µm depending on the lens magnification. The measurements are performed with immersion optics (100x/N.A.1,3, Zeiss Jena) that yields a total optical magnification of 3500fold. The noise-limited sensitivity is h_{min} = 0.5 nm, the acquisition time is determined by the clock frequency of 1000 Hz or 1 ms per pixel.

III. CELL-BIOLOGICAL APPLICATIONS

A. VISUALIZING INTRACELLULAR FINE STRUCTURES

It is evident from the above description that digital microscopic techniques yield most impressive image improvement in situations where the specimen has either virtually no contrast or emits almost negligible amounts of light.

With VEC-DIC microscopy the image quality is highest in the top cell layer of tissue samples. Out of focus material leads to little deterioration of image quality, except in cases where strongly birefringent or depolarizing material such as large numbers of small particles, latex beads, oil droplets, myelin or birefringent inclusions are in the light path. The VEC techniques allow, however, improved optical penetration of tissue slices or small organisms, especially when anaxial illumination[10,37] or light of very long wavelengths such as near infrared is used.[38] The presence of stains or high-contrast inclusions does not allow the application of contrast enhancement to full extent because the image often gets distorted before the small details become visible. Video enhancement, therefore, is best used with unstained material, such as living cells,[18,20,66-69,] or isolated cytoplasmic extracts.[22,48,70-72]

Using VIM, images can be produced at much lower illumination intensity and with lower concentrations of potentially cytotoxic dyes than previously so that this technique has its greatest promise in vital microscopy where the living cells need to be protected from harmful radiation or chemicals.[19,31-33,44,73-77] For VIM the specimen needs to be thin and as close to 2D as possible. Otherwise out of focus fluorescence would make the use of confocal microscopes[6,7,78] necessary. Figure 8 is an example from an analysis of the dynamic behavior of microtubules labeled by transfection with Green Fluorescent Protein-(GFP)-tagged α-tubulin cDNA.

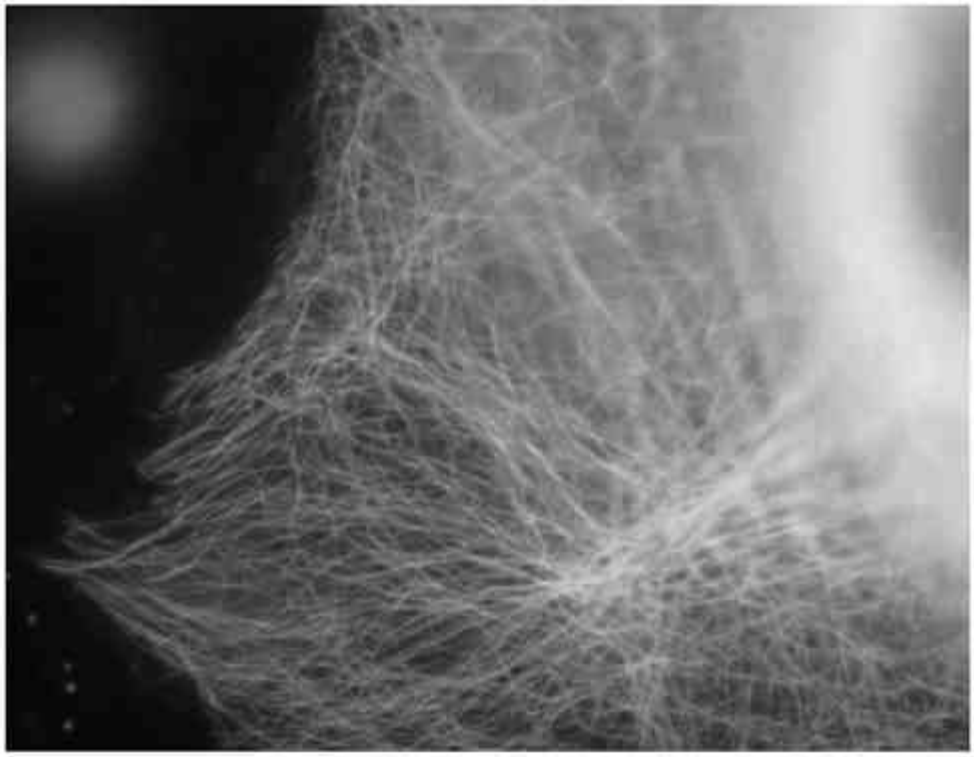

FIGURE 8. Green Fluorescent Protein (GFP) imaging in a living Chinese Hamster ovary (CHO) cell by video-intensified microscopy (VIM). Example from an analysis of the dynamic behavior of microtubules which were for this purpose labeled by transfecting the cell with GFP-tagged α-tubulin cDNA. Microscope, Nikon Eclipse 800; CCD camera, Sensys (Photometrics Inc., Tucson AZ, USA); exposure time, 100 ms; frame width, 40 µm.

It is most advantageous when corresponding pairs of videomicrographs can be obtained[79,80] with one of the images at high resolution with VEC microscopy and one by VIM after addition of vital fluorescent dyes such as organelle-specific markers[16,44,76,81-83] or of fluorescence-labeled antibodies which report the location and amount of all kinds of antigens. The antibodies can be applied after the observation of live cells were completed and the cells fixed. Studies on live cells are, however, equally possible, if cells are microinjected with fluorescent-labelled proteins, transfected with green-fluorescent-protein (GFP)-tagged components, or permeabilized.[75,84- 88] The use of 1 to 5nm colloidal gold-coupled antibodies which are visualized by VEC microscopy in bright-field or epi-polarization mode (Nanovid microscopy) yields non-bleaching images of higher spatial resolution than fluorescence immunocytochemistry or VEC-DIC microscopy.[25,26,89,90] These tagging techniques allow in addition the biochemical or molecular identification of the objects visualized by the VEC techniques.

Fluorescence video micrographs are also well-suited for further quantitative image analysis of fine-morphological parameters. Although little work has been done with organelle morphometry, typical morphometric parameters can be derived if a suitable software package is applied to images stained with organelle-specific vital dyes or antibodies for endoplasmic reticulum networks, for the filamentous arrays of cytoskeletal elements (Figure 8) and mitochondria or for spherical organelles such as lysosomes, secretory vesicles, or Golgi apparatus.

The resolving power of Dynamic Phase Microscopy is also considerably better than the classical Raleigh resolution and for suitable objects it is in the order of tens of nanometers.[63,64]

Taken together, we can say that the various digital light microscopy techniques are best suited for applications involving living cells or extruded cytoplasm, and that they are helpful for a better understanding of the cell's physiology,[31-33,76,91,92] biochemistry,[93,94] molecular architecture,[8,74,76,95] or molecular dynamics.[29,75,96-103]

B. ANALYSIS OF INTRACELLULAR MOTILITY

1. Visualization of Moving Objects and Motion Analysis

Considerable progress in the field of cytoplasmic motility and fine structure had to await the advent of digital microscopy and especially of Allen video-enhanced contrast differential interference contrast (AVEC-DIC) microscopy which allows us to see and to study **all** membrane-bounded organelles and the microtubules, together with their motions and interactions. The new technique was quickly used to study one of the most prominent systems of intracellular organelle motion, namely the transport in nerve cell processes (axoplasmic transport). From these and related studies it became clear that organelle motion in higher animal cells proceeds along microtubules[22,23,66] and to some extent also along actin filaments.[21,71,104]

Many more breakthroughs based on these techniques followed, i.e. the finding that microtubules move actively,[22,105,106,] that microtubules display properties of dynamic instability in vivo,[57,96,97,103] that organelles move bidirectionally on a single microtubule,[22,66,105,107] that membranous organelles can switch between microtubules and actin filaments.[71] Using digital light microscopy the force generating enzymes or molecular motors of organelle movements could be isolated.[108-111] All biochemical studies dealing with the three rapidly growing families of motor proteins, namely kinesins, cytoplasmic dyneins and non-conventional myosins, employ digital microscopy-based motion analysis as the only means to detect and assay these enzymes.

In plant cells the role of the filamentous tracks is played by actin filament bundles as could be demonstrated by the video techniques.[18-20,24] Similar studies performed on various forms of cytoplasmic transport and cellular motility improved our understanding of muscle contraction,[112-114] prokaryotic[115,116] and eukaryotic flagellar motion,[117] pigment granule motion,[118,119] and cytoplasmic transport in protozoans,[67,107] to mention only a few examples.

In nerve cells it is now possible to study axonal transport in olfactory axons that are so thin that they cannot be resolved by conventional light microscopy[120] or in larger myelinated and unmyelinated axons.[47,49,50,121,122] Changes in transport to and from regenerating axons and growth cones were reported[123,124] as well as the specific staining and morphological monitoring over months of neuro-muscular endplates with non-toxic fluorescent dyes.[73,125]

With the methods described above the desired variables to describe quantitatively and further analyse the displacement of organelles or microtubules were obtained.[29,30,47,49,52,58,92,96,98]

Quantitative characterization of the motile events in a cell is a good means to describe the cell's physiological situation, because organelle motion is a vital and very basic property of eukaryotic cells. Once this is accomplished the motile situation can also be used as a very sensitive and multi-facetted indicator to characterize cell populations in cyto-pathological, cyto-

pharmacological, and cyto-toxicological studies.[58,126-128] Furthermore, motion analysis of intracellular objects was used successfully to gain more insight into the molecular mechanisms of force generation,[28-30,112,117,129,130] of actin and microtubule mechanics,[131] or of the assembly and disassembly dynamics of cytoskeletal filaments.[57,96,97,98,132,133] For the analysis of the nanometer-size steps of single molecular motor enzymes high resolution position measurements are required which are suitable for statistical noise analysis.[29,30,99,100]

2. Local Macromolecular Dynamics

Phase images can yield additional information on intracellular supramolecular morphology when used with high temporal sampling rate as in Dynamic Phase Microscopy with 1 ms/pixel temporal and better than 100 nm spatial resolutions. Fig 7 is an example of these scanning measurements of a single mitochondrion. If the scanning is performed only along a relatively short scan line, e.g., 500 nm (28 pixels), this would result in a 30 ms temporal resolution. New insight into supramolecular structures seems possible, since measurements of fluctuations of optical path difference indicate a connection with intracellular activity. Measurements of mitochondria, Vero cells, red blood cells and isolated organelles revealed characteristic dominating frequency components, the intensity of which underwent marked changes with sub-wavelength topology. The co-ordinates of prominent intensity fluctuations correspond to active sites in the cytoplasm or nucleus that can be further analyzed. The spatial resolution of these analyses of active sites, which have different specific frequencies ranging from 0.5 to 3 Hz, is not limited by Airy disk size. The spatial correlation of the movement determines also the length or correlation radius of co-operative processes.

Among the studies already performed are the following. The distribution of the fluctuation intensity along the scan-line was measured for enzyme-loaded **liposomes** under ATP stimulation. The spatio-temporal patterns of liposomal fluctuations revealed a spectral pattern with dominating frequency components at approximately 2 and 3 Hz. When **chromatin dynamics** were measured by dynamic phase microscopy, different compartments of the nuclei displayed typical dominating frequency components. This was especially seen in the nucleoli, when different phases of the cell cycle were investigated.[134] The dynamic properties of DNA need to be characterized further. Intense local optical path difference fluctuations, apparently due to cooperative processes were also measured in freshly prepared **mitochondria** in vitro.[135] ATP increased the intensity of low-frequency components and addition of rotenone or the protonophore FCCP resulted in a decrease. We propose that these results can be attributed to a dependence of enzyme fluctuations on the mitochondrial membrane potential.

Since the local optical path difference is an indicator of the refractive index, its fluctuation indicates cooperative dynamic changes of the conformational state of enzyme complexes or enzyme clusters. The width (100-300 nm) and location of the active sites were detected with an accuracy about 50 nm. Since the contribution of a single enzyme molecule to the optically measured activity would be negligible, we attribute the observed spatial correlation and temporal coherence of the fluctuations to cooperative effects connecting the behavior of enzymes closely adjacent to each other. Not only organelles, also DNA or associated enzymes and mitochondrial enzymes showed such highly cooperative processes that were all ATP-dependent.

C. MEASURING BIOCHEMICAL PARAMETERS IN THE LIVING CELL

Microscopes are often considered to be devices that "merely" make pictures of objects. This is certainly not true for digital microscopes which generate images in which the gray or pseudo-color shades encode quantitative physical or chemical parameters of the specimen, such as motion velocity, concentrations, viscosity, birefringence, phase shift, etc. (see Table I). The digital microscope can, therefore, assume features of a spectrophotometer, spectrofluorimeter, photon multiplier etc. Its dynamic range may be more limited than that of some of the other devices mentioned, but this is generally compensated by the advantage that information is yielded not only in a punctual way (cuvette) but rather in two dimensions (x and y), three dimensions (x,y,z, in through focus series, or x, y, concentration), or even in four dimensions (i.e., if video films of spatio-temporal processes are recorded). Multi-color or even true spectral information can be obtained for each pixel if time series of video frames are stored and the time series for each pixel position are subjected to spectral analysis by FFT.[136,137] This allows the simultaneous analysis of 5 or more fluorescent labels and, by a combination of dyes, all human chromsomes can be distinguished spectrally and displayed in different pseudo-color hues.[136]

Since the transfer function of most video cameras used for quantitative microscopy is linear instead of logarithmic as in the case of the human eye and the photographic film,[4,10] the gray-level information in video images can be used more directly to gain information on the relative amounts of fluorescent substances. Absolute values can be obtained by calibration with standard solutions or samples which are imaged at the same instrumental setting as the unknown samples or by making cells permeable for external medium containing a known concentration of dye or ligand.[31,32]

If information on intracellular concentrations is desired, the optical pathlength, i.e. the thickness of the cell at each pixel, needs to be measured in addition to the intensity values. Such optical pathlength images are obtained when cells are loaded with a dye of homogeneous and exclusively intracellular distribution, such as fluorescein diacetate or labeled dextran and then imaged.[31,32,138,139] In this case the image brightness codes for cell thickness in a quantitative way. "Concentration images" can be derived by dividing regular fluorescence intensity or absorption images obtained with monochromatic light by such “optical pathlength images”. In such measurements the living cell is, so to speak, converted into the biochemist´s measuring cuvette.[140]

At present a rapidly expanding application of digital microscopy in cell biology is the use of fluorescent chelators to measure concentrations of ions and their transient changes. These specially designed dyes cross the plasma membrane in the form of their more lipophilic acetoxymethyl esters and are trapped in the cell after intracellular cleavage of the ester bond. In the case of the Ca^{2+} chelator FURA2 and some related ion indicators, the binding of the ion causes a concentration-dependent spectral shift of the chelator dye fluorescence. By dividing the images obtained at two different wavelengths and with the use of a calibration curve (ratio values of a standard series plotted vs. concentration) one obtains an image containing the concentration information (ratio imaging).[31,32,76,138,141] This procedure is independent of the optical pathlength so that no knowledge of the cell thickness is required. Besides the concentration of Ca^{2+} also H^+ (pH-value), Mg^{2+}, Cl^-, K^+ and Na^+ concentrations can be determined with suitable dyes.[44,76,138,142,143] Image processors can also be programmed to synchronize the filter changer and to display the ion concentration in the form of color-coded images. The temporal resolution

of this technique can be less than one second, and if images are processed offline, data collection is possible even at video rates.

Similar to the above-mentioned extraction of coordinates from series of video frames, one can also extract intensity values of individual image points or image regions from such video series, so that concentration changes in individual cells or in subcellular regions can be followed over time (temporal analysis).[143-145] This makes studies on intracellular transfer, intracellular exchange and metabolism of compounds possible.

Based on these techniques improved assays for regional and temporal enzyme activity could be developed, i.e., for enzymes that consume or synthesize absorbing or fluorescent compounds.[146] Direct luminescence-based enzymatic substrate measurements have been introduced for lactate, glucose and ATP in unfixed tissue sections. The cells or cryosections are permeabilized (e.g. frozen and thawed) and exposed to the coupled enzyme system containing luciferase and suitable bioluminescent substrates and then imaged by photon counting[93,94] (Figure 9). An elegant technique was introduced by Langridge and collaborators to visualize gene expression in plant cells and zebrafish embryos.[147-149] In rhizobium-infected soybean root nodules or in cross sections of tobacco plants the control of gene expression by specific promoters could be directly visualized by the enzyme luciferase introduced into the plant genome as reporter gene. Light emission, i.e. activation of the promoter and expression of its associated genes was quantitated throughout the plant, in cambium cells, or in defined subcellular regions.[147,148]

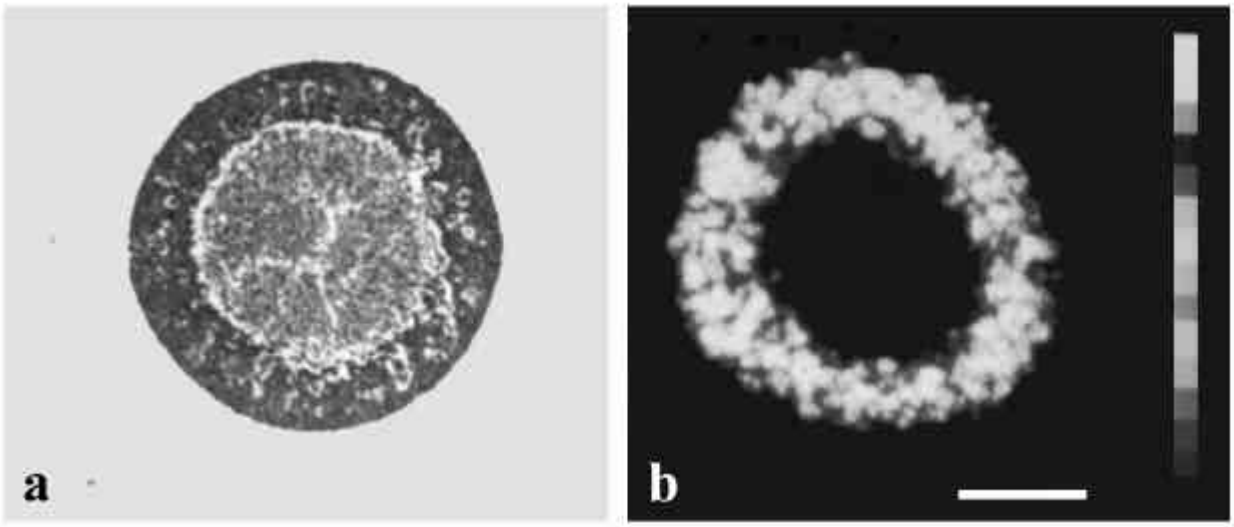

FIGURE 9. Application of the quantitative bioluminescence technique of regional ATP-measurement by photon counting imaging to a cryostat section through a multicellular EMT6 tumor cell spheroid. (a) Unstained cryostat section. (b) Pseudo-color-coded bioluminescence intensity distribution representing the local distribution of ATP concentrations. The color code (right) spans the concentration range from 0.1 to 1.2 mM ATP. Bar 500 µm. Courtesy of W. Müller-Klieser.

The introduction of Green Fluoresent Protein (GFP) from jellyfish that can be employed as protein expression marker is one of the most significant recent advances in electronic light microscopy of living cells.[85,87] A major strength of GFP is that temporal dynamics of identified molecules can be observed and measured using time-lapse imaging. GFP as an expression marker reveals not only protein synthesis in real time in vivo. GFP can also be employed as a

dynamic marker for organelles and other subcellular structures. In combination with digital light microscopy GFP can be used to study intracellular protein trafficking and vesicle transport.[88,91,92] If different spectral variants of GFP are used, dynamic changes in the co-distribution of two components can be investigated within a living cell. GFP variants can also be utilized in the technique of fluorescence resonance energy transfer (FRET)[150] to study protein-protein interaction in vivo without the use of micro-injecting fluorescently labelled proteins; thereby allowing biochemical studies within a living cell.[101] Possibly, GFP can be used for designing also quantitative assays of polypeptide concentrations and dynamics.

IV. CONCLUSION

Digital light microscopy allows us to go beyond the limits of conventional light microscopy. It enables us to see smaller objects than before, to work at lower light intensities, and to generate contrast were none could be generated by conventional techniques. Most of the new techniques and their applications yield best image improvement with unstained specimens so that live cells and their cytoplasm becomes amenable to study. As often in science, new technologies bring new insight, so that already a large body of knowledge on cell structure and function could be accumulated that profoundly changed our static, electron microscopy-based understanding of the cytoskeleton and of cellular structures to a more lively, highly dynamic view. Video microscopists are presently extending the microscope's imaging power well into the molecular domain, making us eyewitnesses also of molecular dynamics, transport and metabolism in the living cytoplasm.

ACKNOWLEDGMENTS

The development of video-microscopic techniques in the authors' laboratories was supported by Deutsche Forschungsgemeinschaft DFG Innovations-Kolleg „Komplexe und Zelluläre Sensorsysteme“ INK-27 and Schwerpunktprogramm “Neue mikroskopische Methoden” (We790/14), Hamamatsu Photonics K.K., Japan, and Ministerium für Bildung, Wissenschaft und Kultur Mecklenburg-Vorpommern. The valuable advice and help of Willi Maile and the members of the “Center for Biological Visualization Techniques” at the University of Rostock is gratefully acknowledged. We thank T. Holstein and W. Mueller-Klieser for their permission to reproduce images from their work.

REFERENCES

1. **Shotton, D.,** The current renaissance in light microscopy. I. Dynamic studies of living cells by video enhanced contrast microscopy, *Proc. Roy. Microsc. Soc.*, 22, 37, 1987
2. **Webb, W.W.,** Light microscopy - a modern renaissance, *Ann. N.Y. Ac. Sci.,* 483, 387, 1986
3. **Weiss, D.G.,** Visualization of the living cytoskeleton by video-enhanced microscopy and digital image processing, *J. Cell Sci., Suppl.* 5, 1, 1986
4. **Inoué, S. and Spring, K.R.** *Video Microscopy. The Fundamentals*, 2nd Ed., Plenum Press, New York, 1997
5. **Inoué, S., and Inoué T.D.,** Computer-aided stereoscopic video reconstruction and serial display from high-resolution light-microscope optical sections, *Ann. N.Y. Acad. Sci.,* 483, 392, 1987
6. **Shotton, D.**, Ed., *Electronic Light Microscopy. The Principles and Practice of Video-Enhanced Contrast, Digital Intensified Fluorescence, and Confocal Scanning Light Microscopy.* Wiley-Liss, New York, 1993
7. **Matsumoto, B.**, Ed., Cell Biological Application of Confocal Microscopy. *Meth. Cell Biol.,* 38, 1993

8. **Allen, R.D.,** New observations on cell architecture and dynamics by video-enhanced contrast optical microscopy, *Ann Rev. Biophys. biophys. Chem.*, 14, 265, 1985
9. **Shotton, D.M.,** Review: Video-enhanced light microscopy and its applications in cell biology, *J. Cell Sci.*, 89, 129, 1988
10. **Weiss, D.G., Maile, W., Wick, R.A., and Steffen, W.** Video microscopy, In *Light Microscopy in Biology. A Practical Approach*, 2nd Ed., A.J. Lacey, Ed., Oxford University Press, 1999, 73
11. **Weiss, D.G.,** Video-enhanced contrast microscopy. In *Cell Biology: A Laboratory Handbook*, Celis, J.E., Ed., 2nd Ed., Vol. 3, Academic Press, San Diego, 1998, 99
12. **Allen, R.D., Travis, J.L., Allen, N.S., and Yilmaz, H**., Video-enhanced contrast polarization (AVEC-POL) microscopy: A new method applied to the detection of birefringence in the motile reticulopodial network of *Allogromia laticollaris*, *Cell Motil*., 1, 275, 1981
13. **Allen, R.D., Allen, N.S., and Travis, J.L.,** Video-enhanced contrast, differential interference contrast (AVEC-DIC) microscopy: A new method capable of analyzing microtubule-related motility in the reticulopodial network of *Allogromia laticollaris*, *Cell Motil*., 1, 291, 1981
14. **Allen, R.D., and Allen, N.S.,** Video-enhanced microscopy with a computer frame memory, *J. Microscopy*, 129, 3, 1983
15. **Weiss, D.G., and Maile, W.,** Principles and applications of video-enhanced contrast microscopy, In *Electronic Light Microscopy: The Principles and Practice of Intensified Fluorescence, Video-Enhanced Contrast and Confocal Scanning Optical Microscopy*, D. M. Shotton, Ed., Wiley-Liss, New York, 105, 1993
16. **Lee, C., and Chen, L.B.,** Behavior of endoplasmic reticulum in living cells, *Cell*, 54, 37, 1988
17. **Allan, V. and Vale, R.D.,** Movement of membrane tubules along microtubules in vitro: evidence for specialised sites of motor attachment. *J. Cell Sci*., 107, 1885, 1994
18. **Lichtscheidl, I.K., and Weiss, D.G.,** Visualisation of submicroscopic structures in the cytoplasm of *Allium cepa* inner epidermal cells by video-enhanced contrast light microscopy, *Eur. J. Cell Biol.*, 46, 376, 1988
19. **Quader, H., Hofmann, A., and Schnepf, E.,** Shape and movement of the endoplasmic reticulum in onion bulb epidermis cells: Possible involvement of actin, *Eur. J. Cell Biol.*, 44, 17, 1987
20. **Allen, N.S., and Brown, D.T.,** Dynamics of the endoplasmic reticulum in living onion epidermal cells in relation to microtubules, microfilaments, and intracellular particle movement, *Cell Motil. Cytoskel.*, 10, 153, 1988
21. **Tabb, J.S., Molyneaux, B.J., Cohen, D.L., Kuznetsov, S.A., and Langford, G.M.,** Transport of ER vesicles on actin filaments in neurons by myosin V. *J. Cell Sci.*, 111, 3221, 1998
22. **Allen, R.D., Weiss, D.G., Hayden, J.H., Brown, D.T., Fujiwake, H., and Simpson, M.,** Gliding movement of and bidirectional transport along native microtubules from squid axoplasm: Evidence for an active role of microtubules in cytoplasmic transport, *J. Cell Biol.*, 100, 1736, 1985
23. **Vale, R.D., Schnapp, B.J., Reese, T.S., and Sheetz, M.P.,** Organelle, bead and microtubule translocations promoted by soluble factors from the squid giant axon, *Cell*, 40, 559, 1985
24. **Kachar, B., and Reese, T.S.,** The mechanism of cytoplasmic streaming in Characean algal cells: sliding of endoplasmic reticulum along actin filaments, *J. Cell Biol.*, 106, 1545, 1988
25. **Mizushima, Y.,** Detectivity limit of very small objects by video-enhanced microscopy. *Applied Optics*, 27, 2587, 1988
26. **Lee, G.M.,** Nanovid microscopy. In *Light Microscopy in Biology. A Practical Approach*, Lacey, A.J. Ed., Oxford University Press, 1999, 425
27. **Inoué, S.,** Imaging of unresolved objects, superresolution, and precision of distance measurement with video microscopy, In *Methods in Cell Biology*, D.L. Taylor, Y.L. Wang, Eds., Vol. 30, Chapter 3, Academic Press, San Diego, 1989, 85
28. **Sheetz, M.P., Turney, S., Qian, H., and Elson, E.L.,** Nanometre-level analysis demonstrates that lipid flow does not drive membrane glycoprotein movements, *Nature (Lond.)*, 340, 284, 1989
29. **Mehta, A.D., Rief, M., Spudich, J.A., Smith, D.A., and Simmons, R.M.,** Single-molecule biomechanics with optical methods. *Science*, 283, 1685, 1995
30. **Gelles, J., Schnapp, B.J. and Sheetz, M.P.,** Tracking kinesin-driven movements with nanometre-scale precision, *Nature (Lond.)*, 331, 450, 1988
31. **Parton, R.M. and Read, N.D.,** Calcium and pH imaging in living cells. *In Light Micrscopy in Biology. A Practical Approach*, Lacey, A.J., Ed.,2nd Ed., Oxford University Press, 1999, 221
32. **Silver, R.B.,** Ratio imaging: practical consideration for measuring intracellular calcium and pH in living tissue. *Meth. Cell Biol.*, 56, 237, 1998
33. **Tsien, R.Y.,** Fluorescent indicators of ion concentrations, In *Methods in Cell Biology, Fluorescence Microscopy of Living Cells in Culture, Part B: Quantitative Fluorescence Microscopy - Imaging and Spectroscopy*, Taylor, D.L., Wang, Y.-L., Eds., Academic Press, San Diego, Vol. 30, 1989, 127

34. **Sluder, G. and Wolf, D. E**., Ed., *Video Microscopy. Methods in Cell Biology*, Vol 56, Academic Press, San Diego, 1998
35. **Russ, J. C**. *The Image Processing Handbook*. CRC Press, London, 2nd Ed., 1994
36. **Steffen, W. and Weiss, D.G.** Marktübersicht Biological Imaging. Ein Bild sagt mehr als 1000 Worte. *BioSpektrum*, 5, 118 1999
37. **Kachar, B.,** Asymmetric illumination contrast: a method of image formation for video light microscopy, *Science*, 277, 766, 1985
38. **Dodt, H.-U., and Zieglgänsberger, W.,** Infrared videomicroscopy: a new look at neuronal structure and function. *Trends in Neurosci.*, **537** 453, 1994
39. **Inoué, S.,** Video image processing greatly enhances contrast, quality, and speed in polarization-based microscopy, *J. Cell Biol.*, 89, 346, 1981
40. **Hansen, E. W., Conchello, J. A., and Allen, R. D.**, Restoring image quality in the polarizing microscope: analysis of the Allen video-enhanced contrast method. *J. Optical Soc. of America*, **A5**, 1836, 1988
41. **Shotton**, **D.**, An introduction to digital image processing and image display in electronic light microscopy. In *Electronic Light Microscopy*, Shotton, D., Ed., Wiley-Liss, New York, 1993, 39.
42. **Cardullo, R.A. and Alm, E.J.**, Introduction to image processing. In *Methods in Cell Biology. Video Microscopy*, Sluder, G., Wolf, D.E., Eds., Academic Press, San Diego, 56, 1998, 91
43. **Taylor, D.L., and Wang, Y.-L.,** *Methods in Cell Biology. Fluorescence Microscopy of Living Cells in Culture, Part A.* Academic Press, San Diego, Vol. 29, 1989
44. **Haugland, R.P.,** *Handbook of Fluorescent Probes and Research Chemicals*, 6th Ed.. Molecular Probes, Eugene, OR, 1996
45. **Lange, B. M. H., Sherwin, T., Hagan, I. M., and Gull, K.,** The basics of immunofluorescence video microscopy for mammalian and microbial systems. *Trends in Cell Biol*., **5,** 328, 1996
46. **Oshiro, M.,** Cooled CCD versus intensified cameras for low-light video-applications and relative advantages. *Methods Cell Biol.*, 56, 45, 1998
47. **Weiss, D. G., Keller, F., Gulden, J., and Maile, W.,** Towards a new classification of intrcellular particle movement based on quantitative analysis. *Cell Motil. Cytoskel.*, **6**, 128, 1986
48. **Brady, S.T., Lasek, R.J. and Allen, R.D.,** Fast axonal transport in extruded axoplasm from squid giant axon, *Science*, 218, 1129, 1982
49. **Weiss, D.G., Galfe, G., Gulden, J., Seitz-Tutter, D., Langford, G.M., Struppler, A., and Weindl, A.,** Motion analysis of intracellular objects: trajectories with and without visible tracks, In *Biological Motion. Lecture Notes in Biomathematics*, Vol. 89, Alt, W., Hoffmann, G., Eds., Springer Verlag, Berlin, , 1990, 95
50. **Weiss, D.G., Langford, G.L., Seitz-Tutter, D., Gulden, J., Keller, F.**, Motion analysis of organelle movements and microtubule dynamics, In *Structure and Functions of the Cytoskeleton, Colloque INSERM* Vol. 171, Rousset, B.A.F. Ed., John Libbey Eurotext, Paris London, 1988, 363
51. **Alt, W. and Hoffmann, G.,** Eds., *Biological Motion. Lecture Notes in Biomathematics*. Vol. 89, Springer Verlag, Berlin, 1990
52. **Tvarusko, W., Bentele, M., Misteli, T., Rudolf, R., Kaether, C., Spector, D.L., Gerdes, H.H., and Elis, R.** Time-resolved analysis and visualization of dynamic processes in living cells. *Proc. Natl. Acad. Sci. U.S.A.*, 96, 7950, 1999
53. **Langford, G.M., Allen, R.D., and Weiss, D.G.,** Substructure of sidearms on squid axoplasmic vesicles and microtubules visualized by negative contrast electron microscopy, *Cell Motil. Cytoskel.*, 7, 20, 1987
54. **Wong M.Y.,** Likelihood estimation of a simple linear regression model when both variables have error, *Biometrika*, 76, 141, 1989
55. **Koles, Z.J., McLeod, K.D. and Smith, R.S.,** The determination of the instantaneous velocity of axonally transported organelles from filmed records of their motion, *Can. J. Physiol. Pharmacol.*, 60, 670, 1982
56. **Koles, Z.J., McLeod, K.D. and Smith, R.S.**, A study of the motion of organelles which undergo retrograde and anterograde rapid axonal transport in Xenopus, *J. Physiol. (Lond.)*, 328, 469, 1982
57. **Weiss, D.G., Langford, G.M., Seitz-Tutter, D., and Keller, F.,** Dynamic instability and motile events of native microtubules from squid axoplasm, *Cell Motil. Cytoskel.*, 10, 285, 1988
58. **Breuer A.C., Lynn M.P., Atkinson M.B., Chou S.M., Wilbourn A.J., Marks K.E., Culver J.E., and Fleegler E.J**., Fast axonal transport in amyotrophic lateral sclerosis, An intra-axonal organelle traffic analysis, *Neurology*, 37, 738, 1987
59. **Cooley, J.W., and Tukey, J.W.,** An algorithm for the machine calculation of complex Fourier series, *Math. Comp.*, 19, 297, 1965
60. **Tychinsky V., Norina S., Odintsov A., Popp F., and Vyshenskaya T.** Optical Phase Images of Living Micro-Objects. *Proc. SPIE Conf. Cell and Biotissue Optics* 2100**,** 129, 1993

61. **Tychinsky V., Kufal G., Odintsov A., and Vyshenskaja T.**, Optical phase imaging of living micro-objects, *Proc. SPIE Conf.* 2008, 160, 1993
62. **Tychinsky V., Kufal G., Vyshenskaya T., Perevedentzeva E., and Nikandrov S.** The measurements of submicrometer structures with the Airyscan laser phase microscope, *Quantum Electronics*, 27, 735, 1997
63. **Tychinsky V., Tavrov A., Shepelsky D., and Shuchkin A.,** The experimental evidence the phase object super-resolution, *Pisma GTPh* 17, 80, 1991
64. **Tychinsky V.,** Microscopy of sub-wavelength structures, *Uspechi Physicheskich Nauk* 166**,** 1219, 1996; *Physics-Uspekhi,* 39, 1157, 1996
65. **Tychinsky V., Masalov I.,.Pankov V., and Ublinsky D.,** Computerized phase microscope for investigation of submicron structures, *Opt. Commun.*, 74, 37, 1989
66. **Hayden, J.H., and Allen, R.D.,** Detection of single microtubules in living cells: Particle transport can occur in both directions along the same microtubule, *J. Cell Biol.*, 99, 1785, 1984
67. **Travis, J.L., and Bowser, S.S**., Optical approaches to the study of foraminiferan motility, *Cell Motil. Cytoskel.*, 10, 126, 1988
68. **Taylor, D.L.**, Centripetal transport of cytoplasm, actin, and the cell surface in lamellipodia of fibroblasts, *Cell Motil. Cytoskel*., 11, 235, 1988
69. **Yeh, E., Skibbens, R.V., Cheng, J.W., Salmon, E.D., and Bloom, K.,** Spindle dynamics and cell cycle regulation of dynein in the budding yeast, *Saccharomyces cerevisiae***.** *J. Cell Biol*., 130, 687, 1995
70. **Weiss, D.G., Meyer, M., and Langford, G.M.,** Studying axoplasmic transport by video microscopy and using the squid giant axon as a model system, *In Squid as Experimental Animals*, Gilbert, D.L., Adelman jr., W.J., Arnold, J.M., Eds., Plenum Press, 1990, 303
71. **Kuznetsov, S.A., Langford, G.M., and Weiss, D.G.,** Actin-dependent organelle movement in squid axoplasm. *Nature (Lond.)*, 356, 722, 1992
72. **Steffen, W., Karki, S., Vaughan, K.T., Vallee, R.B., Holzbaur, E.L.F., Weiss, D.G., and Kuznetsov, S.A.**, The involvement of the intermediate chain of cytoplasmic dynein in binding the motor complex to membranous organelles of *Xenopus* oocytes. *Molec. Biol. Cell*, 8, 2077, 1997
73. **Purves, D., and Voyvodic, T.,** Imaging mammalian nerve cells and their connections over time in living animals, *Trends in Neurosci.*, 10, 398, 1987
74. **Waterman-Storer, C.M., Sanger, J.W., and Sanger, J.M.**, Dynamics of organelles in the mitotic spindles of living cells: membrane and microtubule interactions. *Cell Motil. Cytoskel.*, 26, 19, 1993
75. **Wang, Y.-L.,** Fluorescent analog cytochemistry: tracing functional protein components in living cells, in Methods in Cell Biology, Vol. 29, Chapter 1, Taylor,D.L., Wang, Y.L. Eds., , Academic Press, San Diego, 1989
76. **DeBiasio, R., Bright, G.R., Ernst, L.A., Waggoner, A.S., and Taylor, D.L.,** Five-Parameter Fluorescence Imaging: Wound Healing of Living Swiss 3T3 Cells, *J. Cell Biol.*, 105, 1613, 1987
77. **Whitaker, M.,** Fluorescence imaging in living cells. In: *Cell Biology: A Laboratory Handbook*, 2nd Ed., Celis, J.E., Ed., Vol. 3, Academic Press, San Diego, 1998, 121
78. **Shaw, P.J.,** Introduction to confocal microscopy. In *Light Microscopy in Biology. A Practical Approach*, 2nd Ed., Lacey, A.J., Ed., Oxford University Press, 1999, 45
79. **Demaurex, N., Romanek, R., Rotstein, O.D., and Grinstein, S.,** Measurment of cytosolic pH in single cells by dual-exitiation fluorescence imaging: Simultaneous visualisation using differential interference contrast optics. In *Cell Biology: A Laboratory Handbook*, 2nd Ed., Vol. 3, Celis, J.E., Ed., Academic Press, San Diego, 1998, 380
80. **Foskett, J.K.,** Simultaneous Nomarski and fluorescence imaging during video microscopy of cells. *Am. J. Physiol.*, 255, 566, 1988
81. **Terasaki, M.,** Labeling of the endoplasmic reticulum with $DiOC_6(3)$. In *Cell Biology: A Laboratory Handbook*, 2nd Ed., Vol. 2, Celis, J.E., Ed., Academic Press, San Diego, 1998, 501
82. **Pagano, R.E., and Martin, O.C.,** Use of fluorescence analogs of ceramide to study the Golgi apparatus of animal cells. In *Cell Biology: A Laboratory Handbook*, 2nd Ed., Vol. 2,. Celis, J.E., Academic Press, San Diego, 1998, 507
83. **Poot, M.,** Staining of mitochondria. In: *Cell Biology: A Laboratory Handbook*, 2nd Ed., Vol. 2, Celis, J.E., Ed., Academic Press, San Diego, 1998, 513
84. **Schöpke, C, and Fauquet, C.M.,** Introduction of materials into living cells. In *Light Microscopy in Biology. A Practical Approach*, 2nd Ed., Lacey, A.J., Ed., Oxford University Press, 1999, 373
85. **Chalfie, M., Tu, Y., Euskirchen, G., Ward, W.W., and Prasher, D.C.,** Green fluorescent protein as a marker for gene expression. *Science* 263, 802, 1994
86. **Rizzuto, R., Brini, M., De Giorgi, F., Rossi, R., Heim, R., Tsien, R.Y., and Pozzan, T.,** Double labelling of subcellular structures with organelle-targeted GFP mutants in vivo. *Curr. Biol.* 6, 183, 1996
87. **Chalfie, M. and Kain, S.**, *GFP, Green Fluorescent Protein: Strategies and Applications.* John Wiley and Sons, New York, 1996

88. **Wacker, I., Kaether, C., Kromer, A., Almers, W., and Gerdes, H.H.,** Microtubule-dependent transport of secretory vesicles visualised in real time with a GFP-tagged secretory protein. *J. Cell Sci.* 110, 1453-1463, 1997
89. **Bajer, A.S., Sato, H., and Mole-Bajer, J.,** Video microscopy of colloidal gold particles and immuno-gold labelled microtubules in improved rectified DIC and epi-illumination, *Cell Struct. Funct.*, 11, 317, 1986
90. **De Brabander, M., Nuydens, R., Geerts, H., Nuyens, R., Leunissen, J., and Jacobson, K.**, Using nanovid microscopy to analyse the movement of cell membrane components in living cells, in *Optical Microscopy for Biology*, Herman, B., Jacobson, K., Eds., Wiley-Liss, New York, 1990, 345
91. **Lang, T., Wacker, I., Steyer, J., Kaether, C., Wunderlich, I., Soldati, T., Gerdes, H.H., and Almers, W.,** Ca^{2+}-triggered peptide secretion in single cells imaged with Green Fluoresent Protein and evanescent-wave microscopy. *Neuron*, 18, 857, 1997
92. **Steyer, J.A. and Almers, W.,** Tracking single secretory granules in live chromaffin cells by evanescent-field fluorescence microscopy. *Biophys. J.*, 76, 2262, 1999
93. **Walenta, S., Dötsch, J., and Mueller-Klieser, W.**, ATP concentrations in multicellular tumor spheroids assessed by single photon imaging and quantitative bioluminescence, *Eur. J. Cell Biol.*, 52, 389, 1990
94. **Schwickert, G., Walenta, S., and Mueller-Klieser, W.,** Mapping and quantification of biomolecules in tumor biopsies using bioluminescence. *Experientia* 15, 460, 1996
95. **Hayden, J.H., Allen, R.D., and Goldman, R.D.**, Cytoplasmic transport in keratocytes: Direct visualization of particle translocation along microtubules, *Cell Motil.*, 3, 1, 1983
96. **Seitz-Tutter, D., Langford, G.M., and Weiss, D.G.**, Dynamic instability of native microtubules from squid axons is rare and independent of gliding and vesicle transport, *Exptl. Cell Res.*, 178, 504, 1988
97. **Cassimeris, L., Pryer, N.K., and Salmon, E.D.,** Real-time observations of microtubule dynamic instability in living cells, *J. Cell Biol.*, 107, 2223, 1988
98. **deBeer, E.L., Sontrop, A.M.A.T.A., Kellermeyer, M.S.Z., Galambos, C., and Pollack, G.H**., Actin-filament motion in the in vitro motility assay has a periodic component. *Cell Motil. Cytoskel.* 38, 341, 1997
99. **Qian, H., Sheetz, M.P., and Elson, E.L.,** Single particle tracking (analysis of diffusion and flow in two-dimensional systems). *Biophys. J.* 60, 910, 1991
100. **Saxton, M.J. and Jacobson, K**., Single-particle tracking: applications to membrane dynamics. *Annu. Rev. Biophys. Biomol. Struct.*, 26, 373, 1997
101. **Periasamy, A. and Day, R.N.,** Visualizing protein interactions in living cells using digitized GFP imaging and FRET microscopy. *Meth. Cell Biol.* 58, 293, 1999
102. **Pierce, D.W. and Vale, R.D.** Single-molecule fluorescence detection of green fluorescent protein and application to single-protein dynamics. *Meth. Cell Biol.*, 58, 49, 1999
103. **Sammak, P.J., and Borisy, G.G.**, Direct observation of microtubule dynamics in living cells, *Nature (Lond.)*, 332, 724, 1988
104. **Kuznetsov, S.A. and Weiss, D.G.,** Use of acrosomal processes in actin motility studies. In *Cell Biology: A Laboratory Handbook*, 2nd Ed., Vol. 2, Celis, J.E., Ed., Academic Press, San Diego, 1998, 344
105**. Allen, R.D., and Weiss, D.G.**, An experimental analysis of the mechanisms of fast axonal transport in the squid giant axon, in *Cell Motility: Mechanism and Regulation, 10. Yamada Conference, Sept., 1984, Nagoya*. Ishikawa, H., Hatano, S., Sato, H., Eds, University of Tokyo Press, 1985, 327
106. **Keating,T.J., Peloquin,J.G., Rodionov,V.I., Momcilovic,D., and Borisy,G.G.**, Microtubule release from the centrosome. *Proc. Natl. Acad. Sci. U.S.A.*, 94, 5078, 1997
107. **Koonce, M.P., and Schliwa, M.**, Bidirectional organelle transport can occur in cell processes that contain single microtubules, *J. Cell Biol.*, 100, 322, 1985
108. **Brady, S.T.,** A novel brain ATPase with properties expected for the fast axonal transport motor, *Nature (Lond.)*, 317, 73, 1985
109. **Scholey, J.M., Porter, M.E., Grissom, P.M., and McIntosh, J.R.,** Identification of kinesin in sea urchin eggs and evidence for its localization in the mitotic spindle, *Nature (Lond.)*, 318, 483, 1985
110. **Vale, R.D., Reese, T.S., and Sheetz, M.P.**, Identification of a novel, force-generating protein, kinesin, involved in microtubule-based motility, *Cell*, 42, 39, 1985
111. **Paschal, B.M., Shpetner, H.S., and Vallee, R.B.**, MAP 1C is a microtubule-activated ATPase which translocates microtubules in vitro and has dynein-like properties, *J. Cell Biol.*, 105, 1273, 1987
112. **Yanagida, T. Nakase, M., Nishiyama, K., and Oosawa, F.**, Direct observation of motion of single F-actin filaments in the presence of myosin. *Nature (Lond.)*, 307,58, 1984
113. **Sellers, J.R., and Kachar, B.,** Polarity and velocity of sliding filaments: control of direction by actin and of speed by myosin, *Science*, 249, 406, 1990
114. **Kron, S.J., and Spudich, J.A.,** Fluorescent actin filaments move on myosin fixed to a glass surface, *Proc. Natl. Acad. Sci. U.S.A.*, 83, 6272, 1986

115. **Block, M., Fahrner, K.A., and Berg, H.C.,** Visualization of bacterial flagella by video-enhanced light microscopy. *J. Bacteriol.* 173, 943, 1991
116. **Steinberger, B., Petersen, N., Petermann, H., and Weiss, D.G.,** Movement of magnetic bacteria in time-varying magnetic fields. *J. Fluid Mechanics* 273, 189, 1994
117. **Vale, R.D., Toyoshima, Y.Y.,** Rotation and translocation of microtubules in vitro induced by dyneins from *Tetrahymena* cilia. *Cell*, 52, 459, 1988
118. **McNiven, M.A., and Porter, K.R.**, Microtubule polarity confers direction to pigment transport in chromatophores, *J. Cell Biol.*, 103, 1547, 1986
119. **Rogers, S.L., Tint, I.S., Fanapour, P.C., and Gelfand, V.L.**, Regulated bidirectional motility of melanophore pigment granules along microtubules in vitro. *Proc. Natl. Acad. Sci. U.S.A.*, 94, 3720, 1997
120. **Weiss, D.G. and Buchner, K.,** Axoplasmic transport in olfactory receptor neurons, in *Molecular Neurobiology of the Olfactory System*, Margolis F.L., Getchell T.V., Eds.,. Plenum Publ. Corp., N.Y., 1988, 217
121. **Allen, R.D., Metuzals, J., Tasaki, I., Brady, S.T., and Gilbert, S.P.**, Fast axonal transport in squid giant axon, *Science*, 218, 1127, 1982
122. **Llinás, R., Sugimori, M., Lin, J.-W., Leopold, P.L., and Brady, S.T.,** ATP-dependent directional movement of rat synaptic vesicles injected into the presynaptic terminal of squid giant synapse, *Proc. Natl. Acad. Sci. U.S.A.*, 86, 5656, 1989
123. **Forscher, P., and Smith, S.J.**, Actions of cytochalasins on the organization of actin filaments and microtubules in a neuronal growth cone. *J. Cell Biol.* 10, 1505, 1988
124. **Goldberg, D.J., and Burmeister,D.W.,** Looking into growth cones, *Trends in Neurosci.*, 12, 503, 1989
125. **Herrera, A.A., and Banner, L.R**., The use and effects of vital fluorescent dyes: observation of motor nerve terminals and satellite cells in living frog muscles, *J. Neurocytol.*, 19, 67, 1990
126. **Weiss, D.G.,** Videomicroscopic measurements in living cells: Dynamic determination of multiple end points for in vitro toxicology, *Molec. Toxicol.*, 1, 465, 1987
127. **Maile, W., Lindl, T., and Weiss, D.G.,** New methods for cytotoxicity testing: quantitative video microscopy of intracellular motion and mitochondria-specific fluorescence, *Molec. Toxicol.*, 1, 427, 1987
128. **Geisler, B., Weiss, D.G. and Lindl, T.,** (1996) Video-microscopic analysis of the cytotoxic effects of 2-hydroxyethyl methacrylate in diploid human fibroblasts. *In-vitro Toxicology* 8, 367, 1996
129. **Kishino, A., and Yanagida, T**., Force measurements by micromanipulation of a single actin filament by glass needles, *Nature (Lond.)*, 334, 74, 1988
130. **Kamimura, S., and Takahashi, K.,** Direct measurement of the force of microtubule sliding in flagella, *Nature (Lond.)*, 293, 566, 1985
131. **Felgner, H., Frank, R., and Schliwa, M.,** Flexural rigidity of microtubules measured with the use of optical tweezers. *J. Cell Sci.*, 109, 509, 1996
132. **Mikhailov, A. and Gundersen, G.G.**, Relationship between microtubule dynamics and lamellipodium formation revealed by direct imaging of microtubules in cells treated with nocodazole or taxol. *Cell Motil. Cytoskel.*, 41, 325, 1998
133. **Kurachi, M., Kikumoto, M., Tashiro, H., Komiya, Y., and Tashiro, T.**, Real-time observation of the disassembly of stable neuritic microtubules induced by laser transection: Possible mechanisms of microtubule stabilization in neurites. *Cell Motil. Cytoskel.*, 42, 87, 1999
134. **Vyshenskaja, T.V., Onishchenko, G.E., Petrashchuk, O.M., Tychinsky, V.P., and Nikandrov, S.L.,** Chromatin dynamics measured by phase microscopy in different cell cycle stages *Eur. J. Cell Biol.*, 78, Suppl. 49, 29, 1999
135. **Tychinsky, V.P. Yagudzinsky, L.S., Jean-Francois Leterrier, J.F., Odensjö-Leterrier, M., and Weiss, D.G.,** Real-time measurements of mitochondrial activity using the dynamic phase microscopy method. *Eur. J. Cell Biol.*, 78, suppl. 49, 79, 1999
136. **Schröck, E., du Manoir, S., Veldman, T., Schoell, B., Wienberg, J., Ferguson-Smith, M.A., Ning, Y., Ledbetter, D.H., Bar-Am, I., Soenksen, D., and Ried, Y.G.T.,** Multicolor spectral karyotyping of human chromosomes. *Science*, 273, 494, 1996
137. **Budde, A., Mosenheuer, M., Weiss, D.G. and Gemperlein, R.,** Spectral image analysis in oocytes and cultured cells by a Fourier-interferometric modulated light technique, *Eur. J. Cell Biol.* 78, Suppl. 49, 81, 1999
138. **Giuliano, K.A., Nederlof, M.A., DeBiasio, R., Lanni, F., Waggoner, A.S., and Taylor, D.L.**, Multi-mode light microscopy, in *Optical Microscopy for Biology*, Herman, B., Jacobson, K., Eds., Wiley-Liss, New York, 1990, 543
139. **Luby-Phelps, K., Taylor, D.L., and Lanni, F.**, Probing the structures of cytoplasm, *J. Cell Biol.*, 102, 2015, 1986
140. **Weiss, D.G. and Steffen W.**, Lichtmikroskopie heute: Die lebende Zelle als Meßküvette. *BioSpektrum* 4, 67, 1998

141. **Siegumfeldt, H., Rechinger, K.B., and Jakobsen, M.**, Use of fluorescence ratio imaging for intracellular pH determination of individual bacterial cells in mixed cultures. *Microbiol.* 145, 1703, 1999
142. **Baju, B., Murphy, E., Levy, L.A., Hall, R.D., and London, R.E.,** A fluorescent indicator for measuring cytosolic free magnesium, *Am. J. Physiol*., 256, C540, 1989
143. **Prpic, V., Cowlen, M.S., and Adams, D.O.,** Application of digital imaging microscopy to studies of ion fluxes in murine peritoneal macrophages, In *Optical Microscopy for Biology*, Herman, B., Jacobson, K., Eds., Wiley-Liss, New York, 1990, 337
144. **Wedekind, P., Kubitscheck, U., Heinrich, O., and Peters, R.,** Line-scanning microphotolysis for diffraction limited measurements of lateral diffusion. *Biophys. J*.., 71, 1621, 1996
145. **Wade, M.H., Trosko, J.E., and Schindler, M.,** A fluorescence photobleaching assay of gap junction-mediated communication between human cells, *Science*, 232, 525, 1986
146. **Van Noorden, C.J.F.**, In situ measurements of enzyme reactions. *Eur. Micr. Anal.* 7, 11, 1990
147. **Langridge, W.H.R., Fitzgerald, K.J., Koncz, C., Schell, J., and Szalay, A.A.,** Dual promoter of *Agrobacterium tumefaciens* mannopine synthase genes is regulated by plant growth hormones, *Proc. Natl. Acad. Sci. U.S.A.*, 86, 3219, 1989
148**. Langridge, W.H. and Szalay, A.A.**. Bacterial and coelenterate luciferases as reporter genes in plant cells. *Meth. Mol. Biol.*, 82, 385, 1998
149. **Mayerhofer, R., Araki, K., and Szalay, A.A.,** Monotoring of spatial expression of firefly luciferase in transformed zebrafish. *J. Biolumin. Chemilumin.*, 10, 271, 1995
150. **Bastiaens, P.I.H. and Jovin, T.M.**, Fluorescence resonance energy transfer microscopy. In *Cell Biology: A Laboratory Handbook*, 2nd Ed., Vol. 3, Celis, J.E., Ed., Academic Press, San Diego 1998, 136
151. **Brown, A.F., and Dunn, G.A.,** Microinterferometry of the movement of dry matter in fibroblasts. J. Cell Sci., 93, 56, 1989
152. **Montag, M., Wild, A., Spring, H., and Trendelenburg, M.F.**, Visualization of chromatin arrangement in giant nuclei of mouse trophoblast by videomicroscopy and laser scanning microscopy, In Nuclear Structure and Function, Harris, J.R and Zbarsky, J.B., Eds., Plenum Press, New York, 1990, 272
153. **Forscher, P., Kaczmarek, L.K., Buchanan, J., and Smith, S.J.,** Cyclic AMP induces changes in distribution and transport of organelles within growth cones of *Aplysia* bag cell neurons. *J. Neurosci.*, 7, 3600, 1987
154. **Petermann, H., Weiss, D.G., Bachmann, L., and Petersen, N.,** Motile behaviour and measurement of the magnetic moment of magnetotactic bacteria in rotating magnetic fields, in Biological Motion, Lecture Notes in Biomathematics, Vol. 89, W. Alt und G. Hoffmann eds., Springer-Verlag Berlin, 1990, 387
155. **Gross, D., and Loew, L.M.,** Fluorescent indicators of membrane potential: microspectrofluorometry and imaging, In *Methods in Cell Biology*. Vol. 30, Chapter 7, D.L. Taylor, Y.L. Wang eds., Academic Press, San Diego, 1989, 193
156. **Obaid, A.L., Koyano, T., Lindstrom, J., Sakai, T., and Salzberg, B.M.,** Spatiotemporal pattern of activity in an intact mammalian network with single-cell resolution: optical studies of nicotinic activity in an enteric plexus. *J. Neurosci.*, 19, 3073, 1999
157. **Mitchison, T. J., Sawin, K.E., and Theriot, J.A.**, Caged fluorescent probes for monitoring cytoskeletn dynamics. In *Cell Biology: A Laboratory Handbook* 2nd Ed., Vol. 2, Celis, J.E., Ed., Academic Press, San Diego, 1998, 127

Authors' full addresses:

Axel Budde, Center for Biological Visualization Techniques, Institute for Cell Biology and Biosystems Technology, Department of Biological Sciences, University of Rostock, 18051 Rostock, Germany. Present address: HaSoTec GmbH, Hardware & Software Technology, Burgwall 20, 18055 Rostock, Germany

Walter Steffen, Center for Biological Visualization Techniques, Institute for Cell Biology and Biosystems Technology, Department of Biological Sciences, University of Rostock, 18051 Rostock, Germany

Vladimir P. Tychinsky, Moscow State Institute for Radioengineering, Electronics and Automation, MIREA, Vernadskii Prospect 78, Moscow 117454, Russia

Dieter G. Weiss, Institute for Cell Biology and Biosystems Technology, Department of Biological Sciences, University of Rostock, 18051 Rostock, Germany. Tel. 0381 498 1919, Fax 0381 498 1918, e-mail: dieter.weiss@biologie.uni-rostock.de

---